ΠΑΝΕΠΙΣΤΗΜΙΟ ΘΕΣΣΑΛΙΑΣ

ΣΧΟΛΗ ΘΕΤΙΚΩΝ ΕΠΙΣΤΗΜΩΝ

ΤΜΗΜΑ ΠΛΗΡΟΦΟΡΙΚΗΣ ΜΕ ΕΦΑΡΜΟΓΕΣ ΣΤΗ ΒΙΟΙΑΤΡΙΚΗ

Μελέτη και πρόταση βελτίωσης των ρομποτικών βραχιόνων για εγχειρήσεις

Ζαγόρη Σοφία

ΠΤΥΧΙΑΚΗ ΕΡΓΑΣΙΑ

Επιβλέπων

Κακαρούντας Αθανάσιος

Λαμία, 2021

ΠΑΝΕΠΙΣΤΗΜΙΟ ΘΕΣΣΑΛΙΑΣ

ΣΧΟΛΗ ΘΕΤΙΚΩΝ ΕΠΙΣΤΗΜΩΝ

ΤΜΗΜΑ ΠΛΗΡΟΦΟΡΙΚΗΣ ΜΕ ΕΦΑΡΜΟΓΕΣ ΣΤΗ ΒΙΟΙΑΤΡΙΚΗ

Μελέτη και πρόταση βελτίωσης των ρομποτικών βραχιόνων για εγχειρήσεις

Ζαγόρη Σοφία

ΠΤΥΧΙΑΚΗ ΕΡΓΑΣΙΑ

Επιβλέπων

Κακαρούντας Αθανάσιος

Λαμία, 2021

Με ατομική μου ευθύνη και γνωρίζοντας τις κυρώσεις [(1)], που προβλέπονται από της διατάξεις της παρ. 6 του άρθρου 22 του Ν. 1599/1986, δηλώνω ότι:

1. *Δεν παραθέτω κομμάτια βιβλίων ή άρθρων ή εργασιών άλλων αυτολεξεί **χωρίς να τα περικλείω σε εισαγωγικά** και χωρίς να αναφέρω το συγγραφέα, τη χρονολογία, τη σελίδα. Η αυτολεξεί παράθεση χωρίς εισαγωγικά χωρίς αναφορά στην πηγή, είναι λογοκλοπή. Πέραν της αυτολεξεί παράθεσης, λογοκλοπή θεωρείται και η παράφραση εδαφίων από έργα άλλων, συμπεριλαμβανομένων και έργων συμφοιτητών μου, καθώς και η παράθεση στοιχείων που άλλοι συνέλεξαν ή επεξεργάσθηκαν, χωρίς αναφορά στην πηγή. Αναφέρω πάντοτε με πληρότητα την πηγή κάτω από τον πίνακα ή σχέδιο, όπως στα παραθέματα.*

2. *Δέχομαι ότι η αυτολεξεί **παράθεση χωρίς εισαγωγικά**, ακόμα κι αν συνοδεύεται από αναφορά στην πηγή σε κάποιο άλλο σημείο του κειμένου ή στο τέλος του, είναι αντιγραφή. Η αναφορά στην πηγή στο τέλος π.χ. μιας παραγράφου ή μιας σελίδας, δεν δικαιολογεί συρραφή εδαφίων έργου άλλου συγγραφέα, έστω και παραφρασμένων, και παρουσίασή τους ως δική μου εργασία.*

3. *Δέχομαι ότι υπάρχει επίσης περιορισμός στο μέγεθος και στη συχνότητα των παραθεμάτων που μπορώ να εντάξω στην εργασία μου εντός εισαγωγικών. Κάθε μεγάλο παράθεμα (π.χ. σε πίνακα ή πλαίσιο, κλπ), προϋποθέτει ειδικές ρυθμίσεις, και όταν δημοσιεύεται προϋποθέτει την άδεια του συγγραφέα ή του εκδότη. Το ίδιο και οι πίνακες και τα σχέδια*

4. *Δέχομαι όλες τις συνέπειες σε περίπτωση λογοκλοπής ή αντιγραφής.*

Ημερομηνία:**26/09/2021**

Η δηλούσα

Ζαγόρη Σοφία

Μελέτη και πρόταση βελτίωσης των ρομποτικών βραχιόνων για εγχειρήσεις

Ζαγόρη Σοφία

Τριμελής Επιτροπή:

Κακαρούντας Αθανάσιος, Αναπληρωτής Καθηγητής (επιβλέπων), Τμήμα Πληροφορικής με Εφαρμογές στη Βιοϊατρική

Τασουλής Σωτήριος, Επίκουρος Καθηγητής, Τμήμα Πληροφορικής με Εφαρμογές στη Βιοϊατρική

Καρανίκας Χαράλαμπος, Λέκτορας, Τμήμα Πληροφορικής με Εφαρμογές στη Βιοϊατρική

Περίληψη

Η υποβοηθούμενη από ρομπότ ελάχιστα επεμβατική εγχείρηση (Robot-Assisted Minimally Invasive Surgery – RAMIS) είναι μια καινοτομία που έχει ωφελήσει εκατοντάδες χιλιάδες ασθενείς μέχρι σήμερα. Περιλαμβάνει τον χειρισμό ρομποτικών βραχιόνων από τον χειρουργό και τους βοηθούς του με σκοπό τη δημιουργία μικρών τομών και μιας σχεδόν αναίμακτης χειρουργικής διαδικασίας.

Τα μηχανήματα έχουν γίνει εργαλεία επαγγελματιών υγείας και, με την προσθήκη αισθητήρων, προσφέρουν μετρήσεις που τους καθοδηγούν στα στάδια της διαδικασίας. Τα πλεονεκτήματα από τη χρήση τους είναι πολλά και όμως δεν είναι τόσο δημοφιλή όσο θα περίμενε κανείς. Πολλοί επαγγελματίες υγείας πιστεύουν ότι τα χειρουργικά ρομπότ δεν τους δίνουν τόσα σχόλια όσο οι ανθρώπινες αισθήσεις τους και μπορεί να διστάζουν να τα χρησιμοποιήσουν. Το υψηλό κόστος αυξάνει τις αμφιβολίες τους.

Το σύστημα ανατροφοδότησης αφής (haptic feedback) είναι πολύ σημαντικό για την ομαλή διεξαγωγή της εγχείρησης. Ωστόσο ελάχιστα μηχανήματα διαθέτουν μέτρηση της δύναμης με την οποία οι λαβίδες του βραχίονα γραπώνουν και ακόμα λιγότερα δίνουν στοιχεία για το είδος της επιφάνειας που ακουμπούν τα εργαλεία. Έτσι, όχι μόνο δυσχεραίνεται η πρόσβαση του ειδικού στον οργανισμό, όχι μόνο αυξάνεται ο κίνδυνος τραυματισμών του ασθενούς, αλλά και παραβλέπονται πληροφορίες που θα ήταν χρήσιμες στη διάγνωση παθήσεων.

Στην παρούσα εργασία παρουσιάζεται η ανάπτυξη ενός συστήματος ανίχνευσης υφών ικανό να ενσωματωθεί σε ρομποτικούς βραχίονες που μετέχουν σε χειρουργικές διαδικασίες. Με βάση την τεχνολογία τριβοηλεκτρικότητας και πιεζοηλεκτρικότητας και αξιοποιώντας ανοιχτό υλικό και λογισμικό υλοποιήθηκε μια λύση που είναι βιοσυμβατή, μικρή σε μέγεθος και χαμηλή σε κόστος.

Λέξεις κλειδιά: Ενσωματωμένα συστήματα, υποβοηθούμενη από ρομπότ ελάχιστα επεμβατική εγχείρηση, αισθητήρες (RAMIS), αισθητήρες, τριβοηλεκτρκότητα, πιεζοηλκτρικότητα, βιοπληροφορική, βιοϊατρική μηχανική, Arduino

Abstract

Robot-assisted Minimally Invasive Surgery (RAMIS) is an innovation that has benefited hundreds of thousands of patients to date. It involves the manipulation of robotic arms by the surgeon and their assistants so as to create small incisions and an almost bloodless surgical process.

Machines have become the tools of health professionals and, with the addition of sensors, offer measurements that guide them through the stages of the process. The advantages from their use are many and yet they are not as popular as one would expect. Many health professionals feel that surgical robots don't give them as much feedback as their human senses and they can be hesitant to use them. The high cost adds to their doubts.

Haptic feedback in particular is crucial for the the smooth conduction of the operation. However, few machines have a measure of the force with which the arm forceps grip and none, to our knowledge, give information about the type of surface the tools touch. This not only makes it difficult for the surgeon to access the body, not only increases the risk of injury to the patient, but also overpasses information which would be useful in diagnosing diseases.

In this graduation thesis we present the development of a texture detection and applied force measurement system suitable for integration onto robotic arms involved in surgical procedures. Based on the technology of triboelectricity and piezoelectricity and utilizing open-source hardware and software, a solution was implemented that is biocompatible, small in size and low-priced.

Keywords: Embedded systems, laparoscopy, minimally invasive surgery, robot-assisted minimally invasive interventional surgery (RAMIS), sensors, triboelectricity, piezoelectricity, bioinformatics, biomedical engineering, Arduino

Acknowledgments

Without the support and trust of certain people this graduation thesis wouldn't have been possible. First, I would like to thank my supervisor, Kakarountas Athanasios, for tirelessly offering me guidance and sharing my enthusiasm for this project. Our collaboration has been a great learning experience. I would also like to express my gratitude to my parents who always believe in me and help me achieve my goals. Finally, I give thanks to the engineers who contribute to free open source software and hardware, making technology accessible to everyone.

Table of contents

Table of figures

Table of tables

1. Introduction

The technological advances of the recent decades could not but affect the health sector. Health professionals now use machines in every aspect of their work. For the facilitation of diagnosis and treatment they receive accurate measurements, images from inside the body, the levels of substances in the blood and other useful values. Thanks to the development of Telemedicine, it is not necessary for a patient and a health professional to be in the same space for medical reports to be created. In the treatment of patients, electronic devices complete procedures such as blood dialysis and chemotherapy.

Machines assisting in surgical operations are the latest innovations in the Health technology field. Because of their many advantages, medical facilities quickly adopted them. The number of patients operated on with the help of robots is increasing every year and their use is now routine. The scientific community is now looking for improvements in this kind of devices and ways to make them accessible to even the less equipped health facilities.

In this thesis our goal was to build a system that reflected the needs of the scientific community. For us, the best system is small in size and volume, increases the efficiency of the robot and is economical enough to be easily obtained by any medical unit. At the same time, we do not want it to complicate the robot's handling, but to guide a health professional of any level with simple signals.

The structure of this project is as follows. Chapter 2 studies robotic surgery and the use of tactile technologies. This chapter identifies general features of the technology and makes a case for deficiencies. Chapter 3 provides a thorough study of the available medical solutions in robotic surgery and presents a detailed table with their characteristics. In chapter 4 the requirements of the system are examined, whereas chapter 5 covers the design of a pilot implementation. The system evaluation follows in chapter 6, where the results of the sensors testing are displayed. Chapter 7 are discussed the final conclusions, a quality evaluation of the Thesis, as well as future developments and improvements. In Annex A the Arduino codes are listed.

2. Haptics in Nature and Technology

2.1 Defining touch and texture

Understanding this concept is crucial, as measurement of touch and strength is essential in laparoscopic surgery and in the diagnosis by a health professional. Humans calculate these values empirically and our goal is for the machines that assist in surgical operations to acquire it as well.

The sense of touch in humans is the perception of the texture of an object from the surface of the skin.

Texture is defined as a continuation of features on a surface with or without the existence of a pattern. It can be detected in many dimensions and depends on the scale at which it is observed. In objects close to the human scale, a feature larger than the surface of a finger is not considered part of the texture. As the scale increases, the difference might be less and less detected. For instance, mountain ranges may not be presented as significant differences on the surface of the Earth when observed from space.

Some descriptions of texture are "hard" / "soft", "rough" / "smooth", "slippery" / "sticky". These result from skin contact with the corresponding surface. Upon contact, the skin is deformed by friction with the microstructure of the object, causing electrical activity in the nervous system. Eventually this activity is decoded and categorized by the brain as one of the aforementioned categories.

For humans, roughness is the most important value, but it cannot be clearly defined. It has been observed that when the irregularities on a surface are thinner, the higher irregularities are more noted than the short ones. But when they are wider, the height does not matter. Their factor of the height should not be overlooked. For instance, in larger spaces the irregularities give a greater feeling of roughness when they are sparsely met.

The hardness of an object is measured in terms of the resistance it exerts when it comes in contact with another object that tries to penetrate, deform or wear it down.

2.2 The laparoscopic surgery

The surgical method of laparoscopy involves opening a small incision in the patient and performing an operation in the same or a nearby area. The incision can be half to one and a half centimeters in diameter and its size varies depending on the area to be operated on. From the incision surgical instruments (forceps, scissors, etc.) are inserted, as well as a camera with a mounted light. The camera transmits images to a screen monitored by a healthcare professional. This type of operation is considered

very discreet. It leaves smaller wounds on the body and precipitates recovery significantly. We must note that even in the case of laparoscopic surgery the doctor must grasp, push aside and manipulate large organs such as the spleen, liver, kidney and bladder.

Figure 1: Laparoscopy with and without the use of robots [1]

2.3 The concept of robot-assisted surgery

In recent years, the work of health professionals has been facilitated by surgical robots, which carry laparoscopes and tubes or arms with surgical instruments. They consist of a console, from which they are manipulated, the body with arms that enter the patient, and a screen from which an image is transmitted from inside the patient. Surgeons and nurses use them as multi-tools.

Surgical remote controls allow the user to perform surgical operations using a "subordinate robot" in a remote environment by commanding a master robot. There is also bilateral control for the coordination of the two robots. In this case the arms of the surgical robot move without direct human contact, but only through the surgeon's movements from a console.

In some surgical robotic systems, the health professional manually guides the surgical instrument attached to the robotic assistant. The type of telesurgery in which the main operator is next to the subordinate robot mechanical operator is called "hands on".

Many times, the system software creates restrictions that force a robot to move in desired directions or prevent it from moving in restricted areas. Some consider this

method to be faster and safer. This technique is particularly beneficial for palpation, which allows the detection of hard lumps and the definition of surfaces, as observed in artificial models of human organs. [2]

A variety of laparoscopic surgery assisting robots are available in research facilities and the market. There are small variations between models. Sometimes the arms move separately, other times they are members of a larger tower. The arms can also differ in the degrees of movement freedom they have in the three-dimensional space.

Figure 2: The Senhance surgical robot with its three arms and console. © 2021 Asensus Surgical US, Inc.
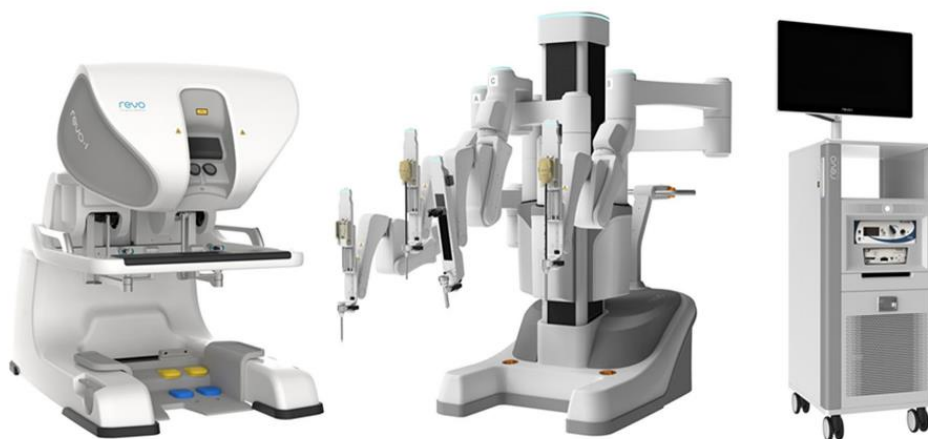
Figure 3: The surgical robot REVO-I with its console, the operating table and the screen cart. © 2021 National Center for Biotechnology Information, U.S. National Library of Medicine.
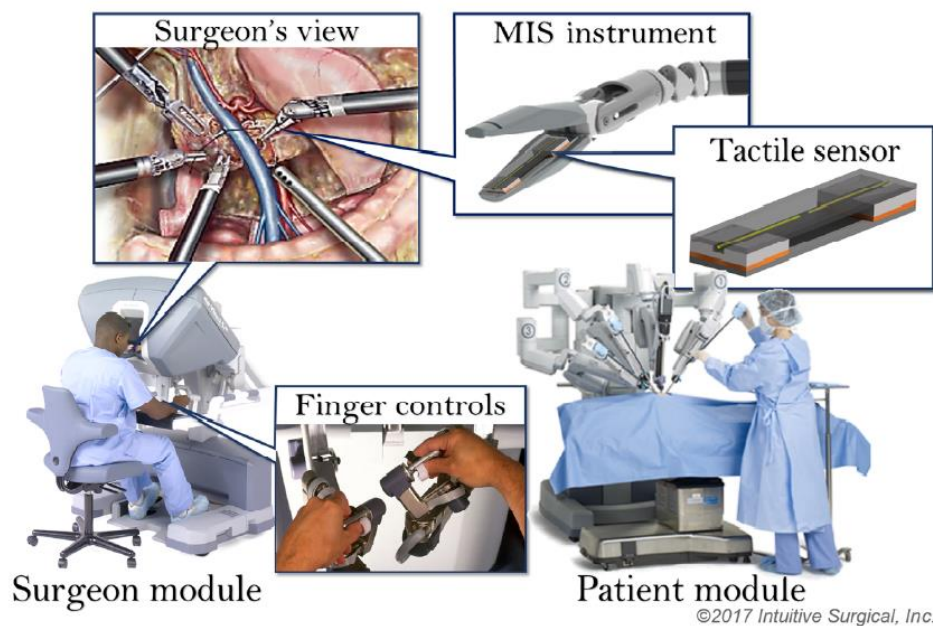
Figure 4: Overview of a surgical robot in an operating environment. The surgeon handles the robot remotely, sitting in front of the console. Surgical instruments are screwed to the ends of the arms. The tactile sensors embedded in the grasps help the surgeon differentiate tissues. © 2017 Intuitive Surgival Inc.

2.3.1 Advantages from the use of robots in surgery

Due to discreet intervention of the robots, the wounds they leave in the body are smaller, guaranteeing a faster patient recovery. Their potential for accuracy adds to the skill of doctors and makes the environment more controllable, reducing the mistakes of the human factor. The learning curve with these machines is short, allowing their immediate introduction to the operating room. The surgeon sits in a comfortable seat during the procedure and their fatigue is reduced over time. Although the controller has some distance from the operating table, his or her involvement is direct. The robotic arms can be moved easily and precisely even in the most delicate processes.

2.3.2 Disadvantages from the use of robots in surgery

Despite its benefits, tactile information is not without challenges. These vary depending on the shape of the robot and the requirements of the user.

The surgical robots offer a plethora of data which the user must consider during the surgery. Many stimuli can lead to sensory overload and make the work more difficult. If the operation requires detailed manipulations, a large number of signals can distract the surgeon.

Moreover, a system designed to interact with soft tissue can be unstable when it comes in contact with a hard surface, such as a bone. The opposite can happen, as well. In these circumstances, the signals on the operator screen will be hard to decipher. The above scenario is unappealing, because the operator will not have a clear picture of what is happening inside the patient.

Another decisive factor is the cost. The increasing prices of sensory instruments is one of the main reasons for the delay of their integration onto surgical robots. [3] Even though innovative machines enter the market every year, medical facilities and health professionals do not have enough resources to procure them. [2] What is more, the presence of many sensory tools is required so that satisfactory values can be extracted. Their ergonomic inclusion in the present robot models might be an issue for the manufacturers.

In addition, each device involved in the operation process must follow some standards of size, durability and sterility for many consecutive minutes. These standards are set by the European Medicines Agency (EMA) in Europe, the US Food and Drug Administration (FDA) in the United States, and similar Organizations in other countries. In order for the manufacturers to comply with the above requirements, they implement costly solutions, which discourage future buyers. The need to build sensory mechanisms that follow specific health industry standards is a technical challenge that many manufacturers cannot overcome.

2.4 The role of haptic feedback in examining biological organs

Palpation of an organ can lead the doctor to conclusions about its condition. [4][5]

Tuberculosis is found in 80% of the lungs due to the high oxygen pressure in the area. A lung affected by tuberculosis is identified by wounds which alter its texture and shape. [6][7] The phenomenon of cavitation and fibrosis (scarring) is observed as well as nodular infiltrates. [8][9] In the palpation of the lungs, large-scale morphology has been shown to be just as important as small-scale morphology. [10]

Hepatic cirrhosis (or Liver cirrhosis) can also be detected by palpation. Exposure to toxins such as alcohol and infections can lead to liver damage. The organ has the ability to repair these wounds and thus scar tissue is created in the area. As time goes on and the damage continues, layers of scar tissue accumulate, changing the overall texture of the organ. [11] The liver hardens and progresses to the cirrhosis condition. Cirrhosis is also caused by chronic hepatitis B, primary biliary cholangitis [12], and even from cardiac cirrhosis. [13]
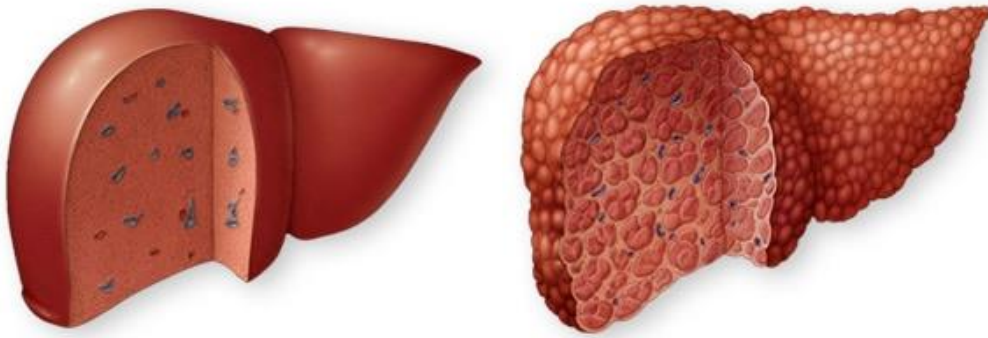
Figure 5: On the right a healthy liver, on the left liver with cirrhosis. © 2021 Mayo Foundation for Medical Education and Research.

Another case where palpation would be helpful is the early stages of pancreatic cancer. It is difficult to detect in the early stages as the organ is located deep in the body and cannot be felt above the skin. Usually, patients show symptoms only when the cancer has grown too much or has spread to other organs [14].

Another example is changes in the texture of the heart, which may soften or harden depending on the patient's condition or lifestyle (cardiomyopathy). [15][16] In the case of myocardial ischemia, the heart muscle dilates, dilates, and weakens. For the causes of cardiomyopathy, a myocardial biopsy is often performed, where small tissue samples are taken from the heart and examined under a microscope.

Finally, analyzing the condition of the tissues may help to identify cancerous tumors, glands and arteries in the body. Palpation tests for breast [17][18], pancreas, prostate and artery [19][20][21]cancer have already been reported.

In no case is the usefulness of imaging through computed tomography and magnetic resonance imaging undermined. Detection through palpation is mentioned since it offers another way of identifying issues in case the patient needs to undergo surgery. Even in the case the surgery does not take place for diagnostic reasons, there is a chance that the health professionals will find themselves in front of health problems which, due to lack of symptoms, are not recorded in the patient's health history.

2.5 Advantages of haptic feedback in robot-assisted surgery

The accuracy with which the movements are made in the operation is enhanced, resulting in a faster operation with fewer internal injuries from human errors. The speed of the operation increases, because internal sensors transmit values from the operation environment and no more incisions need to be made for further investigation of an issue.

With fewer openings, the scars are reduced reducing the patient's pain and the recovery period. The aesthetically better result is important for many patients, as well. If the laparoscopic camera is not able to give an accurate picture due to the presence of liquids or smoke from the electrosurgical surgeries, the indications from the sensory information will guide the surgeon.

The surgeon is given the opportunity to use their knowledge of organ palpation in order to find differences in the tissues. There are cases where layers of healthy tissue cover the problematic areas and the doctor should be able to do that examination. This inspection is important, as it determines what part of the tissue will be cut or when the needle will be inserted. Other times it helps the doctor find how compact an organ is by palpation in order to detect hidden cancerous tumors. [22]

Small parts of the robot can often be inserted into narrow areas where the doctor's fingers could not reach. At these points, sensor indications are required for the operation to proceed safely.

In modern times, virtual reality technology is used in the training of young surgeons. Sensory feedback can be inserted into the console used by the user in the virtual reality environment and contribute to the more realistic preparation of the trainees. [2][23][24]

It is also necessary for the doctor to be aware of how fragile the environment is in order to perform the appropriate movements each time without injuring the patients. The robot provides the necessary values for this evaluation to be achieved.

3 Study of the current technological situation in robot-assisted surgery

3.1 The lack of surgical robots with haptic feedback

Until the completion of this project, no surgical robots with a sense of touch were found. Many of them transmit images from an internal camera and data about the force that tools exert inside the body. The operator's perception could be expanded by adding a sensing system, something none of them are reported to have, according to research. [25], [26], [27], [28], [29], [30], [31], [32], [33], [34], [35], [36], [37], [38], [39] A table of the most well-known robotic systems for surgery on the market follows.

Table 1: Present surgical robots and their haptic feedback

Robot	Company	Touch	Force	No Data
Amadeus RSS	Titan Medical			•
Avatera [40]	Avateramedical		•	
Avicenna Roboflex	Elmed Medical Systems			
Da Vinci System [41], [42], [43], [44]	Intuitive Surgical		•	
Flex	Medrobotics Corp		•	
Hominis™	Memic Innovative Surgery			•
Hugo	Medtronic			•
MASTER	Nanyang Technological University		•	
Mirosurge [45], [46]	German Aeurospace Center DLR		•	
REVO I [47], [48], [49]	Meerecompany		•	
Senhance	TransEnterix		•	
SPORT [50]	TitanMedicalInc			•
SurgiBot	TransEnterix		•	
Verb Surgical	J&J/Alphabet			•
Versius	CMR Surgical		•	
ViaCath	BIOTRONIK		•	

3.2 Triboelectricity and Piezoelectricity

Before moving on, it is necessary to study the concepts of triboelectricity and piezoelectricity as they are considered important for adding an artificial sense of touch to surgical robots. The changes in voltage in triboelectric and piezoelectric applications are used not only for charging the device but as a measurement factor of how the environment affects the system.

3.2.1 Triboelectricity

Triboelectricity is the generation of electricity by contact or separation of two dielectric materials. This polarized interface that is created through that process supplies power devices. For now the scale of those devices is relatively small. [51] [52]

Triboelectric energy nanogenerators – (TENGs) are based on polymers compatible with flexible substrates. Depending on the configuration and materials of the generators, power generation can be achieved in the following ways: a) dielectric to dielectric in vertical contact separation mode, b) metal to dielectric in vertical contact separation mode, c) dielectric to dielectric in lateral slipping, d) metal to dielectric in lateral slipping, rotation function and operation of an electrode.

In "dielectric to dielectric" the transfer of electric charge takes place in the contact of two polymers which is caused by an external force. This approach is used to generate energy from everyday and simple actions such as walking. In "metal to dielectric" the logic is the same but the difference is in the polymers.

Generators that use rotation are based on the frictional load of a material on a plane either by moving it along an axis or by rotating the material around an axis on the same plane. The output of the generator is affected by the frequency of rotation, which can be adjusted according to the requirements for the output.

All of the above are based on two-electrode technology, but the one-electrode technology is equally efficient, especially for finger-touch actions and self-powered systems.

A recent innovation is wearable devices [53] and electronic fabrics, which collect data and energy from direct contact with the user. [54] The latter are textiles based on polyester, silver nanowires and graphene core-shell nanocomposites. [55]

3.2.2 Piezoelectricity

Piezoelectric energy is the electricity that results from pressure and latent heat. Electric charge accumulates in some solid materials with a crystalline structure, such as iron, some ceramics and biological material (bones, DNA and proteins) during

mechanical stress due to the linear electromechanical interaction between the mechanical and electrical states of materials.

With this pressure the structure of the material slightly changes and the balance of positive and negative charges inside it are disturbed, causing an electric charge. The piezoelectric effect is reversible. When a voltage passes through the above materials, the charge balance is restored. [56]

3.2.3 Piezoelectric sensors

The methods for manufacturing piezoelectric sensors depend on the needs they will be called to meet. One of the most common methods is the embroidering of conductive yarn on textile substrates in such patterns that define circuits or circuit elements. When these circuits are created, it is possible to weld on them. There are many types of conductive yarns for this process. Some of these are silver threads, stainless steel threads, titanium, gold, and titanium.

Copper wire is recommended for use in applications where no contact is made with the skin and silver thread where this contact is required. Copper skin exposure can cause dermatitis and other allergic reactions in some users.

Another approach is to coat non-conductive threads with metals, galvanic substances, or minerals. This allows the production of electronic fabrics. Typical fabric coating processes include electrolytic coating, chemical vapor deposition, spraying and conductive polymer coating.

Instead of using conductive yarn, conductive inks can be printed onto non-conductive fabric. These inks are based on highly conductive metals such as silver, copper, gold, and graphene, which is a conductive allotrope of carbon.

It is important to mention the Electronic Skin (e-skin), the surface that covers machines and gives them stimuli from the environment, like the skin of many living multicellular organisms. Recently, e-skin has been developed that collects the energy needed to operate through alternative sources, using piezoelectricity and triboelectricity, among others. [57]
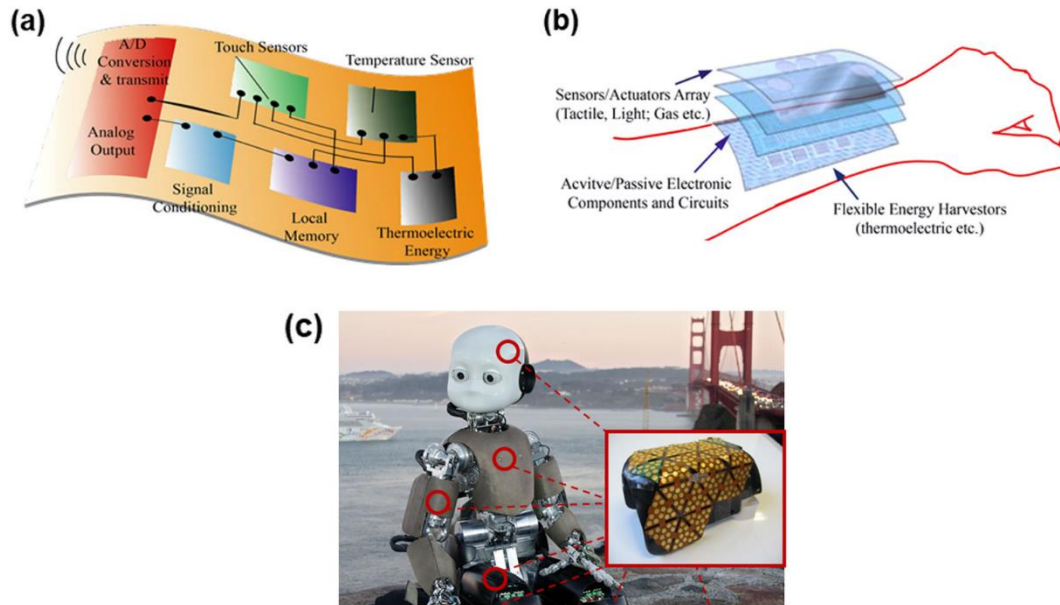
Figure 6: (a) Multi-sensory and flexible electronic skin for robots and humans. Three-dimensional shape of a flexible e-skin with multiple electronic components (sensors, electronic components, memory, power collectors, etc.) distributed along the same surface or (b) stacked. (c) The iCub robot with body and hands covered with electronic leather. © 2019 Springer Nature Limited.

The company Pressure Profile Systems® has manufactured a range of textile flexible pressure sensors. Their sensor, Conformable TactArray, consists of conductive fabric. It maps the pressure points and gives quality values even when it is folded or wrapped. It is considered suitable for wearable electronic products.

Figure 7: The sensor Conformable TactArray. © 2021 Medical Tactile Inc.

The company Eleksen lunched the touchpad ElekTex®, a pressure sensor made of conductive fabric that connects to the company interface and acts as a keyboard, board for painting, and controller for music.

Figure 8: Using ElekTex® for drawing in the company interface. © 2021 Medical Tactile Inc.

Piezoelectric sensors show scalability, linearity, low lag and low noise. What is more, they can operate in both static and dynamic conditions, while maintaining acceptable repeatability. [58] Some disadvantages are high power consumption, as well as occasional be low repeatability and long hysteresis. Making them small enough to maintain their accuracy is another challenge. [59]

3.3 Other touch-sensitive systems for surgery

At the time of the writing of this project, the sensation of touch on robotic machines for surgery is still experimental. The following are research papers related to the subject under study.

Ahmad Abiri et al. [60] report the construction and placement of a sensor on the tip of a Da Vinci surgical robot arm, to detect organic tissue properties, and also the force exerted by the operator on them. The sensor detected the strength and hardness of the materials through vibrations. The sensory instrument was integrated into the inner surface of the forceps.

The scaled normal force feedback was given via a pneumatic balloon contacting the surgeon's fingers. The balloons inflate in accordance with the force value detected by the sensor at the ends of the instrument. So far, the application has not been tested in a patient's body in real conditions, but only on objects.

Figure 9: The sensors mounted on the forceps of the robotic arm. © 2019 Springer Nature Limited.

Naghmeh M. Bandari et al. presented a piezoresistive-optical fibre tactile sensor which they modeled and manufactured themselves. They called it "hybrid", as it also measures the pressure exerted by objects and their hardness/rigidity. [61]

They relied on the principle of piezoelectricity, measuring the voltage created in the gap between the optical fibers when the sensor came in contact with an object. There is a small light in the center of the sensor and its quantity is constantly measured. If an object pushes the sensor, the light passing through the optical fibers will be reduced. Depending on the amount of light it is determined whether the object is soft or hard.
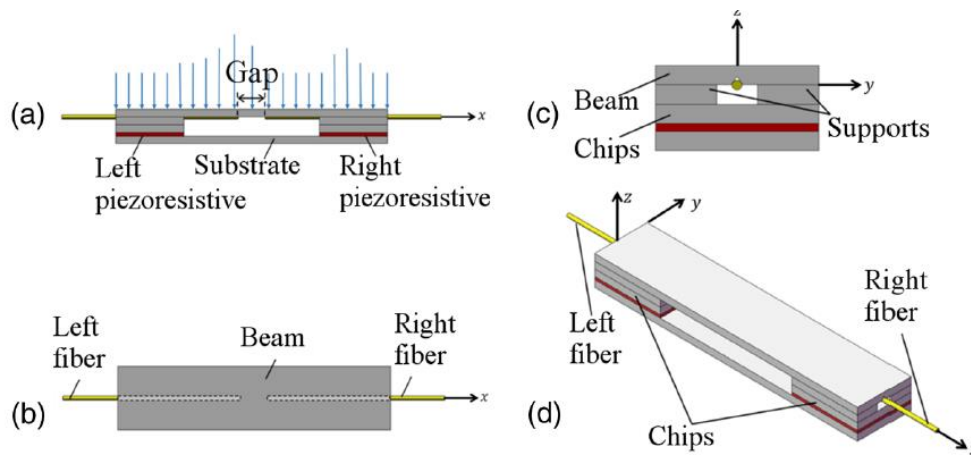
Figure 10: The structure of the hybrid sensor. (a) lateral, (b) top, (c) longitudinal, (d) perspective view. © 2017 National Center for Biotechnology Information, U.S. National Library of Medicine.

There is also the haptic robot Robo-Tac-BMI of Mojra et al [17] for breast mass recognition. The robotic system moves a recessed catheter, guided by a visualization interface. The probe on the catheter mainly consists of a pressure sensor and a touch detection mechanism.

Figure 11: The Robo-Tac-BMI and its parts (© 2011 John Wiley & Sons, Ltd.)

After the catheter comes in contact with the breast, data are extracted on the behavior of the tissue (its viscoelasticity, in particular). The system is capable of detecting

various diseases and tumors in the tissue, as shown in Figure 12. It is designed to be integrated into surgical robots on the market.
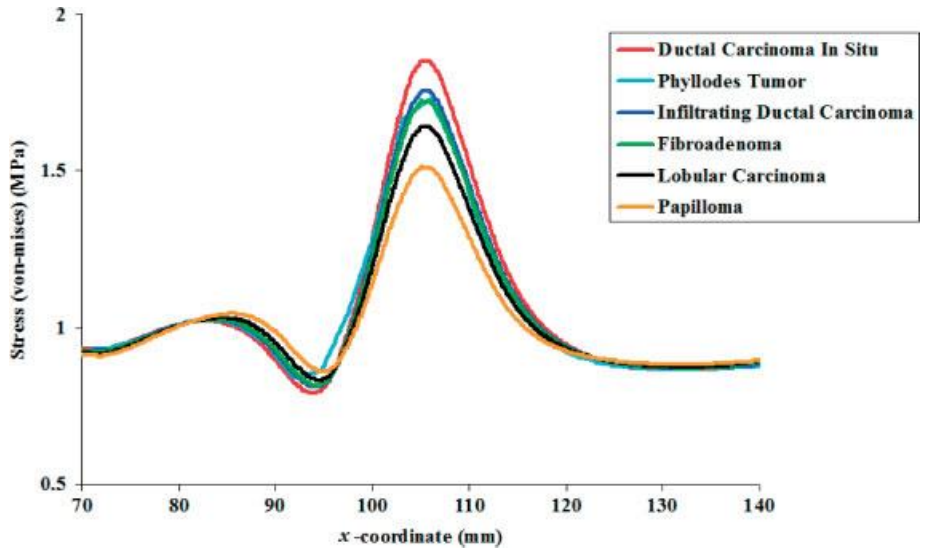
Figure 12: Pressure graph for different mass elasticity values with a stress rate of 1% from the above research. © 2011 John Wiley & Sons, Ltd.

A. Abouei Mehrizi et al. constructed a sensing system which detects and identifies types of arterial stenosis in simulations. [21] The tip of the system touches the surface of the tissue that contains an artery or the surface of an artery. The pressure exerted by the materials on the system is converted into a measurable electrical signal. The electrical signal changes proportionally to the force exerted on the object.
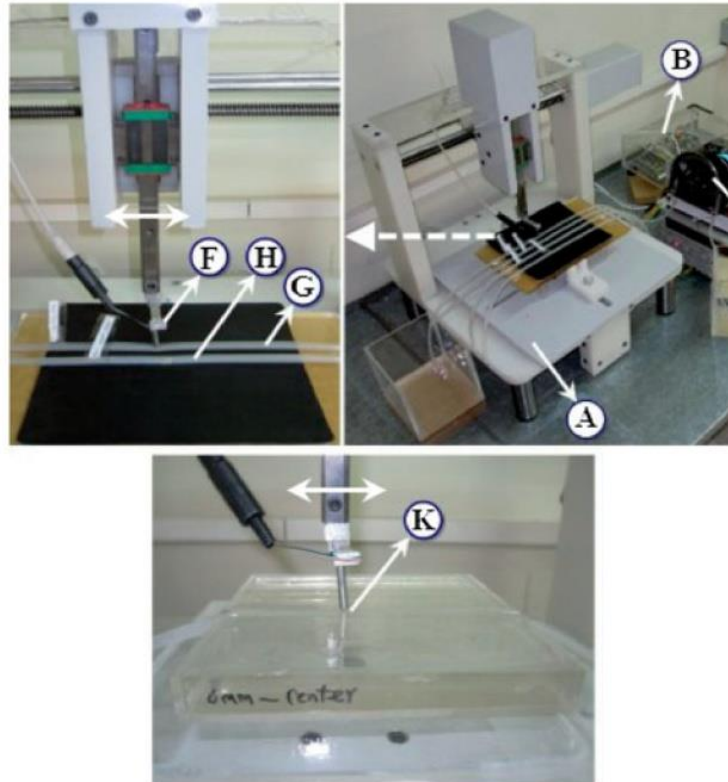
Figure 13: The system during testing. (a) displacement robot, (b) electronic board, (c) peristaltic pump, (d) power supply, (e) water resource, (f) strain gauge load cell, (g) the silicone tube simulating a healthy artery, (h) the silicone tube simulating an artery with 30% stenosis (k) The contact of tactile probe and paraffin gel included a silicone tube.
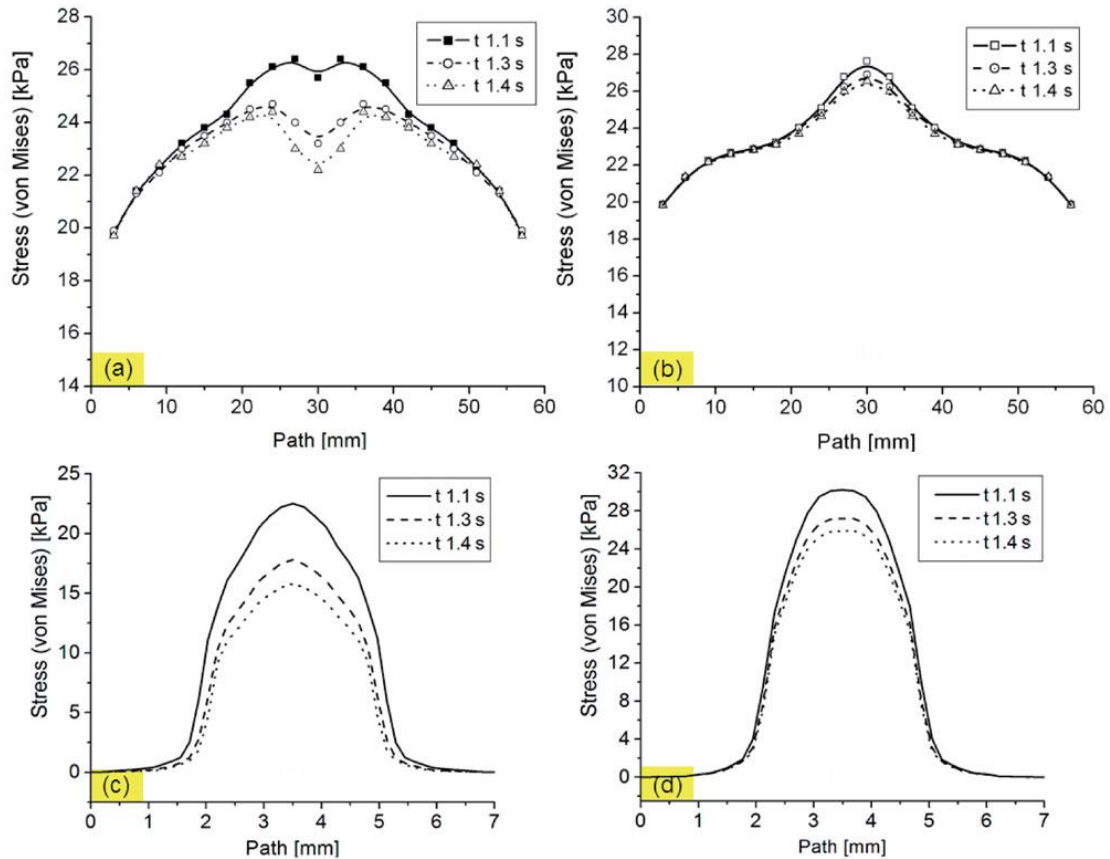
Figure 14: Distribution of pressure on the surface of the tissue and the finger for different models where the artery is located either inside or outside the tissue, for both a healthy artery and an artery with stenosis. © 2014 National Center for Biotechnology Information, U.S. National Library of Medicine.

Yingxuan Zhang et al. [62] built a piezoelectric touch sensor to detect the condition of tissues in robot-assisted surgery. This detection can also be done at an angle of 0 to 45 degrees. The values it shows indicate the hardness of each tissue, as well as the presence of hard masses or tumors. The sensing elements are lead zirconate titanate piezoelectric ceramics. A layer of carbon fiber is in the center of the sensor. The tip of the stainless-steel detector is a sphere that comes in contact with the tissue.
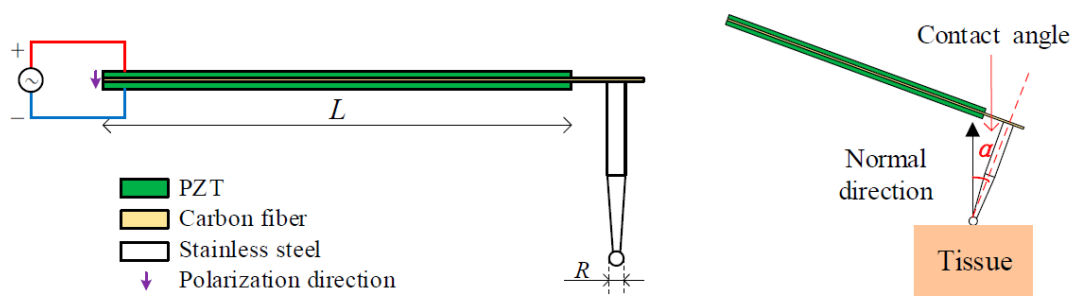
Figure 15: The structure of the piezoelectric tactile sensor and the model of detection in different angles of sensor brobe and tissue (α). © 2020 National Center for Biotechnology Information, U.S. National Library of Medicine.
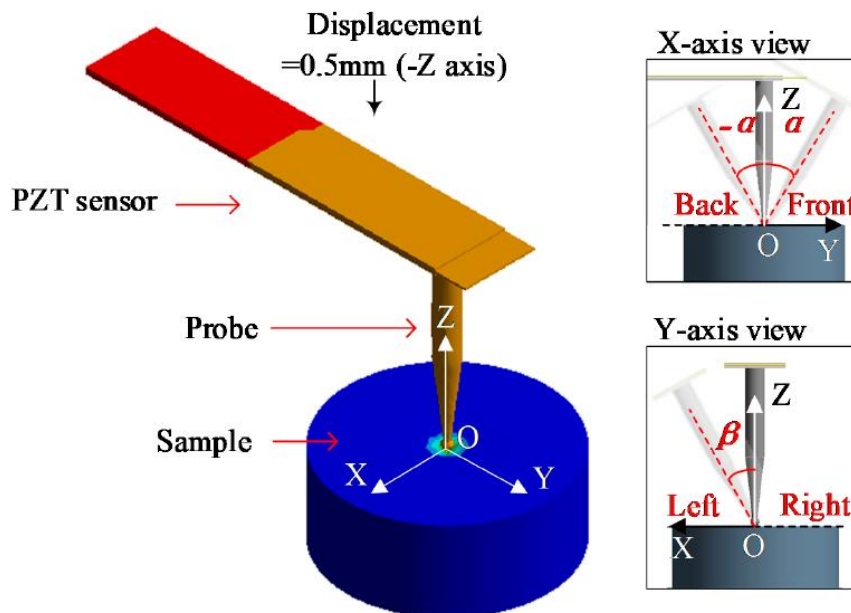
Figure 16: Detection simulation in front, rear, and left view at a predetermined contact angle. © 2020 National Center for Biotechnology Information, U.S. National Library of Medicine.

An AC voltage applied in the opposite direction to the polarization direction of the lead zirconate titanate ceramics causes vibration in the sensor. Mechanical changes caused to the sensor by contact with objects lead to changes in electrical resistance. Consequently, the coordination frequency of the system changes and this is information related to the hardness of the tissue.
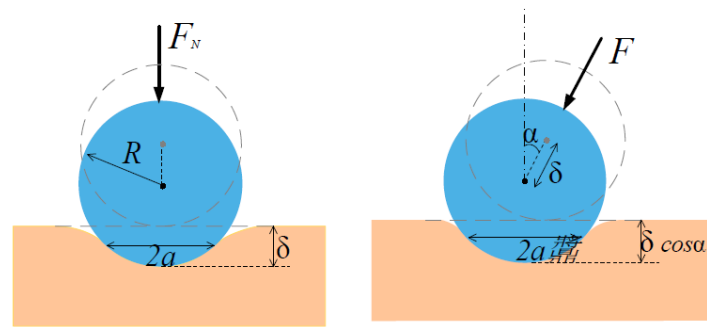
Figure 17: Model of the contact between the sensor tip and the tissue at angle 0 and angle α. © 2020 National Center for Biotechnology Information, U.S. National Library of Medicine.

Yahui Yun et al. [63] also relied on the properties of lead zirconate titanate (PZT). The sensor and the actuator were made of that compound. As in the previous construction the hardness of an object is manifested by the change of frequency. In this application an Archimedean spiral metal sheet is introduced. It keeps the coordination frequency low, while allowing the 10mm sensor to take quality data by converting the vibration of the X axis to the vibration of the Y axis.

The proposed sensor along with a case can be mounted on a robot catheter during surgery. It measures stiffness in the range 0-2 MPa, detects and locates lumps in the tissue.
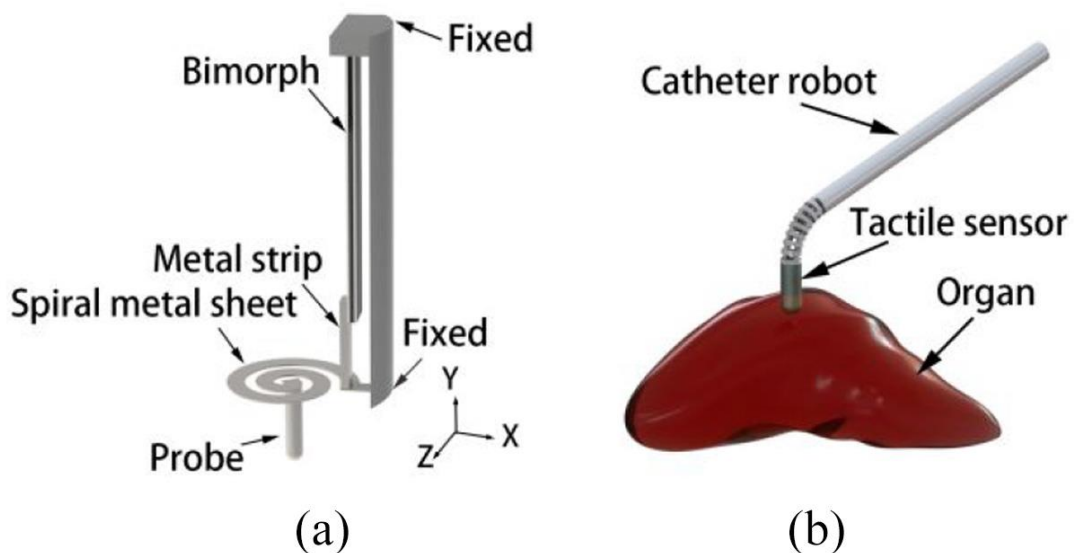
Figure 18: Illustration of the (a) sensor's basic structure and (b) sensor application. © 2019 National Center for Biotechnology Information, U.S. National Library of Medicine.

Marco Beccani et al. [64] created a prototype of a wireless tactile sensor. It is a cylindrical device (15 mm in diameter, 60 mm in length) that can be inserted into the body through a small surgical incision and produce a map of volumetric stiffness

distribution of the area of interest. It will be guided inside the body by the surgeon's hand. Its operation requires first touching the surface of the construction and later the texture map of the area is generated. The surgeon can then manipulate the sensor as a cursor to identify any margins of a harder area buried beneath the tissue.
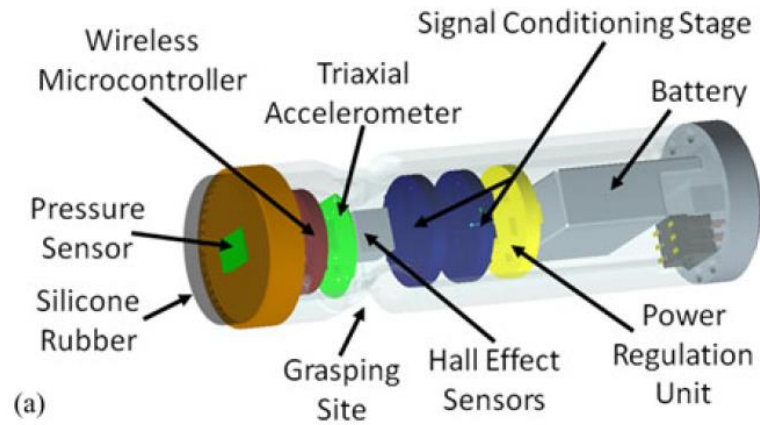
Figure 19: Internal structure of the probe of the prototype. © 2018 IEEE.
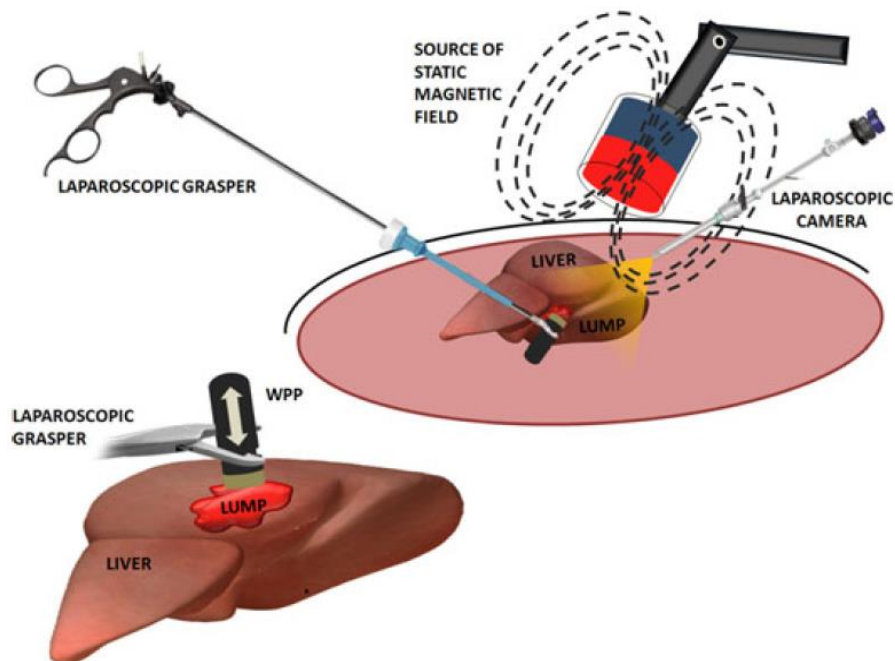
Figure 20: Simulation of the device operating. © 2018 IEEE.

For the creation of the map, data is collected from the barometric pressure sensor, the accelerometer, and the magnetic field sensors. They are received by a wireless microcontroller. A three-axis accelerometer measures the inclination of the magnet and draws its rotation in relation to the global coordinate system.

The user interface accompanying the prototype displays in real time the sensor coordinates, a diagram of the pressure from various areas that were palpated and, in case the pressure has exceeded a threshold, the numerical value of the recess depth. Visual indicators alert the user if the sensor is outside the predefined workspace.

3.4 The technology of conductive fabrics

3.4.1 Conductive fabrics and electronic components

They are either fabrics of natural or plastic yarn which are then coated with conductive materials, or surfaces woven or knitted with flexible metallic yarns. [65] They can be combined with ready-made printed circuits on the market, such as the Intel Xadow board, which are suitable for wearing. Systems from conductive fabric offer low power consumption and high input resistance.

Special plugs and connectors are needed to connect the mechanical parts to the fabric ones. The mechanical parts can be removed, in which case the connections will be made with snap-type joints that are pressed directly on conductive lines. Some of the methods used for creating permanent connection are micro-welding, thermoplastic adhesion, mixed conductive polymer welding, joint welding, and electrolytic coating. For example, conductive threads can be used as cables but connecting them with cables will require soldering with silver paste and possibly some conductive tape for stabilization. [66]

The electronic components can be woven directly as mentioned above or added into special cases attached to the fabric. Hooks and fabric switches help this connection. Since it is possible to coat the fabric with a metal or a conductive polymer, it is possible to form these elements on the fabric this way.

Conductive fabrics can store energy but also become key parts of sensors. In these circumstances, materials such as silicone encapsulate the construction and enhance its structural cohesion. [67], [68]

In **Figure 22** some basic textiles and electronic materials used in electronic textiles are presented. [69]
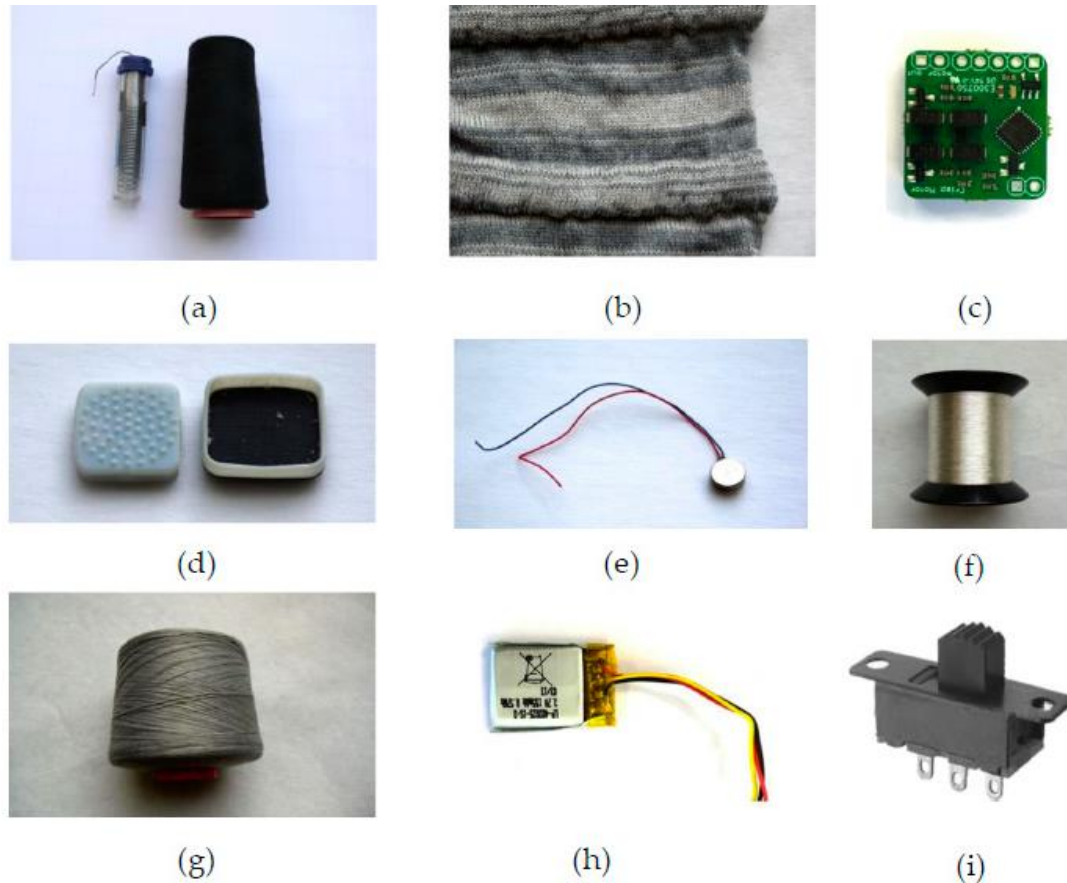
Figure 21: Textile and electronic materials used in e-textiles. (a) Solder and polyester thread, (b) E-textile capacitor, (c) Printed Circuit Board (PCB) for e-textiles, (d) Casing shell, (e) Vibration motor; (f) Elektrisola textile conductive wire; (g) Bekintex conductive thread, (h) Lithium-ion battery used to power e-textiles, and, (i) On/Off Slide switch. © 2018 National Center for Biotechnology Information, U.S. National Library of Medicine.

3.4.2 Textile sensors

Those sensors consist of textile parts attached to electronic components or wires, as mentioned above. There are many studies and constructions of sensors in the scientific literature.

In the capacitive pressure sensors the capacity changes depending on the distance between two conductive parallel plates. The Resistive Pressure Sensors are based on an electrical resistance that increases when the material inside them, usually fabric, is stretched or compressed. [70]

There are also optical sensors that operate based on fluctuations in light intensity or width that can be detected by a photodetector on an optical fiber, which is sewn onto a fabric. Humidity and temperature can be detected with such sensors. Fabric humidity sensors detect the fluctuation of humidity due to the alteration in their conductivity.

Fabric temperature sensors detect water vapor due to the change in dielectric constant inside them.

It is also possible to create fabric-based capacitors. They are governed by the basic principle of capacitors, two plates of compatible conductive materials which are separated by a dielectric. In this case the plates are woven and/or embroidered with conductive thread. The dielectric may be a fabric separator, synthetic foams, and/or a soft non-conductive polymer. [69]

There is also the possibility of a system being made entirely out of fabric. Ziqiang Zhou et al. report the fabrication of a wearable human-computer interactive system where keys, when touched, transmit signals to devices. The system was made on a single silicone substrate. The fabric system was connected by conductive threads to the copper wires that reached the flexible printed circuit board. [71]

3.4.3 The Tribexor system

It detects specific movements of the joints as it is integrated into the user's clothes. Its core is a fabric-based triboelectric sensor. Two fabric slabs in the center collect potential, which is sent by potential collector layers onto the slabs in a multi-stage amplifier circuit. The signal voltage from the friction is amplified and digitized. Noise is rejected and data is transmitted via Bluetooth. The system is protected by shields on the upper and lower surfaces.

The output signal is altered when the environment becomes very humid but it still works satisfactorily when the user sweats. The creators state that waterproof fabric can be used for the system. [72]
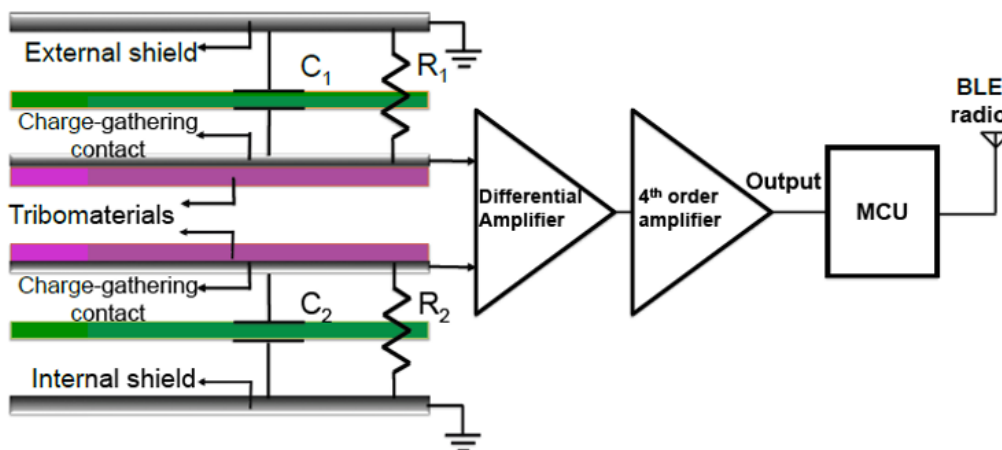
Figure 22: The design of Tribexor. © 2018 NSF Public Access Repository.

3.4.4 A flexible tactile fabric sensor

Ren, J., Wang, C., Zhang, X et al. [73] made this sensor by hot pressing graphene (reduced graphene oxide, or "r-GO" specifically) onto a non-conductive cotton fabric. This application of this technique resulted in the material having very good conductivity and elasticity.
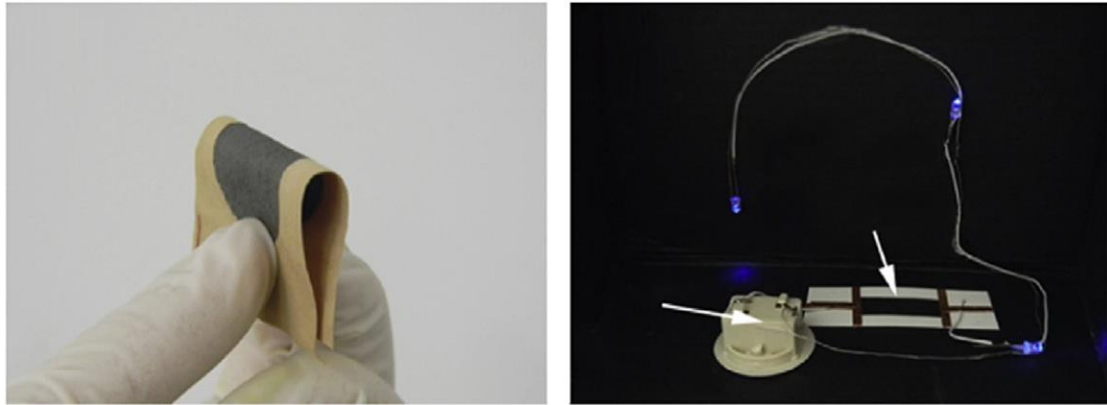
Figure 23: Demonstration of the flexibility and conductivity of the conductive r-GO deposited cotton fabric hot pressed at 180°C for 60 min. © 2017 University of Cambridge.

3.4.5 Textile gas sensor

Ren J, Wang C, Zhang X et al. [73] also made a wearable gas sensor based on textile fiber substrates. The single fibers coated with graphene (r-GO) allow sufficient energy transfer, and flexibility of the material. The clothes can be washed without the capabilities of the sensor being altered. The sensor reacts with nitrogen dioxide at room temperature, acetone, ethanol, ethylene and carbon dioxide.

Figure 24: A RGO gas sensor thread with, made of microfiber bundles (cylinders) wrapped with RGO. (B) Cotton and RGO yarns and RGO polyester yarns. (C) Cotton RGO thread gas sensor system sewn on the fabric. (D) The portable gas detection and alarm system. © 2017 University of Cambridge.

3.4.6 A flexible capacitive pressure sensor

This wearable sensor was made of conductive fabric electrodes and a dielectric layer of silicone microstructure. The dielectric layer is extremely small (less than 1 mm thick). Its base is a microporous silicone elastomer with embedded sugar granules. Salt crystals be used as well. The conductive fabrics are joined to this layer by lamination. Conductive fabric electrodes are utilising heat compression technology and adhesive film technology. [74]
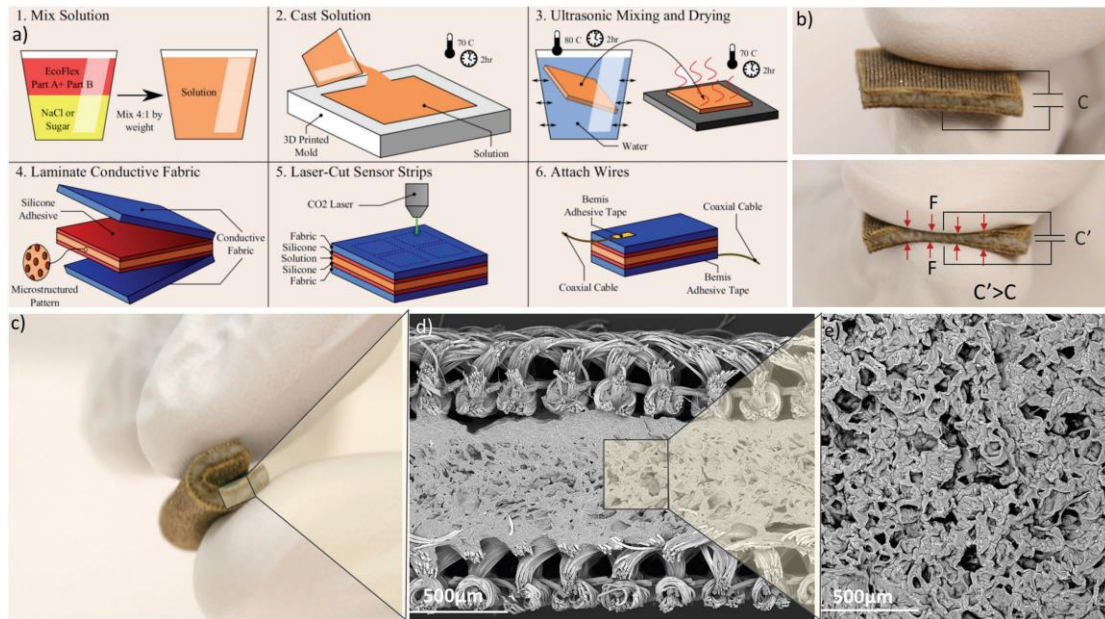
Figure 25: (a) The process of manufacturing the pressure sensor. (b) Actual image of the sensor operating under force load (c) Bending of the sensor. (d) Cross section of the sensor recorded via SEM. (e) SEM image of the sensor. © 2017 John Wiley & Sons, Ltd.

3.5 Electrical textiles for everyday use

The term refers to clothing that incorporates various sensors which allow it to collect data from the environment such as pressure, humidity, temperature, and tension. The presence of a control board is required for the processing of information. such textiles operate by detecting changes when in contact with other surfaces due to the triboelectric effect and electrification.

In the research field of conductive yarns, some important discoveries have been made in recent years, increasing the future capabilities of these sensors. Byungwoo Choi et al. Developed a textile electronic system resistant to moisture and pollution through chemical processes. [75] Some of these fabric systems have antibacterial properties. [76] Zhenhua Tang et al. have reported textile sensors that can be washed along with the clothes in which they are integrated, since they are hydrophobic. Thus, they are cleaned but the water does not damage them. [77] A hydrophobic pressure sensor was also fabricated by Seong Jun Kim et al. [78]

Clothes with integrated sensors have entered the market, as many companies notice the need for more easily accessible technology. One of these companies is Sensoria Inc. It hass developed a "smart sock" which takes values while the user runs through fabric pressure sensors and evaluates whether this exercise strains their foot. Feedback is visualized through via the Sensoria app. Thus, the user has indications on how to improve their technique and maintain the benefits of exercise. T-shirts that record heart rate and transfer data to the application have also been made by the same company. A small Bluetooth device is used for data transfer and is fastened on the blouse.

The protective clothing company Dainese recently launched a "smart jacket" that opens like an airbag. The battery-operated electronic system is located between the fabric layers of the garment. Its seven sensors constantly receive input from the environment. In dangerous conditions such as an abrupt change in height and collision detection with objects and vehicles, the protective parts are activated.

The company Xenoma has a range of smart clothes that follow the technology of printed elastic circuits on fabric. The tactile sensing, the reception and transmission of data on the garment is done mainly through this technology. The construction material of their products is called "e-skin". Some of the company's clothes focus on motion detection and circulatory system health assessment.

The company's latest line, e-skin Sleep & Lounge, is suitable for monitoring elderly patients. The absence of plastic cables and extra devices (apart from a small central one that fits in the top pocket) makes these clothes comfortable and suitable for wearing at home. The system in the clothing alerts health professionals and relatives in case of user fall, or when physical activity levels are low, and also provide information on the elderly person's sleep cycle.

Robotic skin

Yuji Hirai et al. have proposed a skin suitable for robots that will allow them to perceive stimuli like a human. The cover is made of silicone and the interior is made of conductive rubber and conductive fabric. The skin detects patterns and distribution of spatial and temporal pressures. Due to the repetitive pattern in its construction it can be cut and be just as effective in different sizes. [79]
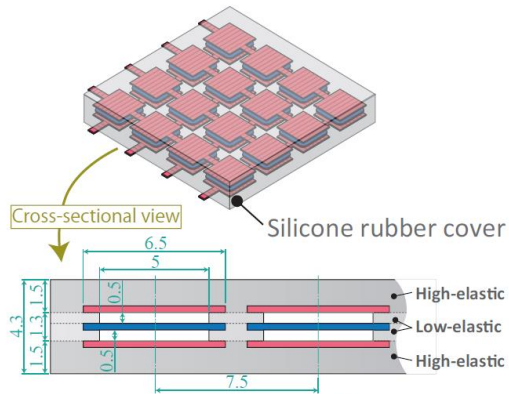
Fig. 3. Structure of the silicone rubber covering the pressure sensitive part (Four layers of silicone rubber sheets with different elasticities are utilized for positioning and upgrading the pressure sensitive part.)
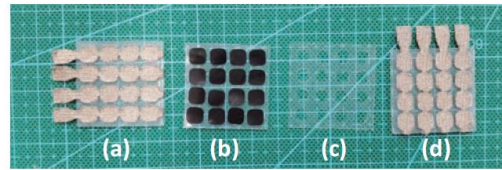
Fig. 4. Fabricated component parts of the pressure sensitive part ((a) 1st silicone layer and the conductive fabric in the lower layer, (b) 2nd silicone layer and the fragments of the pressure-conductive rubber, (c) 3rd silicone layer, and (d) 4th silicone layer and the conductive fabric in the upper layer)
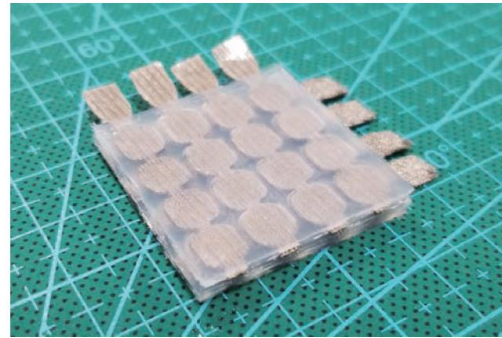
Fig. 5. Constructed 4 × 4 matrix configuration of the tactile sensors array

Figure 26: The robotic skin. © 2018 IEEE.

Xi Duan et al. used a piezoelectric cloth to map the points of touch on a prototype for a robotic skin, as shown in Figure 27. [80]
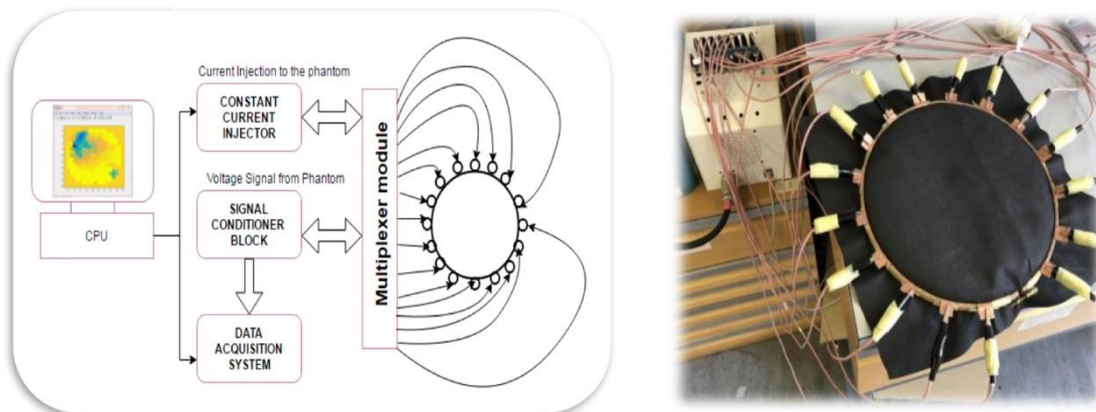
Figure 27 (© 2019 National Center for Biotechnology Information, U.S. National Library of Medicine)

Electrical impedance tomography (EIT) is used to recreate an image of a conductivity distribution within the test object, namely the conductive cloth. EIT systems measure limit voltages according to constant, low frequency and multiple infusion currents. The software is capable of produce cross-sectional images of the conductivity distribution across the textile surface.

Another surface that feels pressure like human skin was proposed by Chen D et al. They built a surface with pressure sensors, where each sensor consisted of a piezoelectric material between two copper pads. [81]
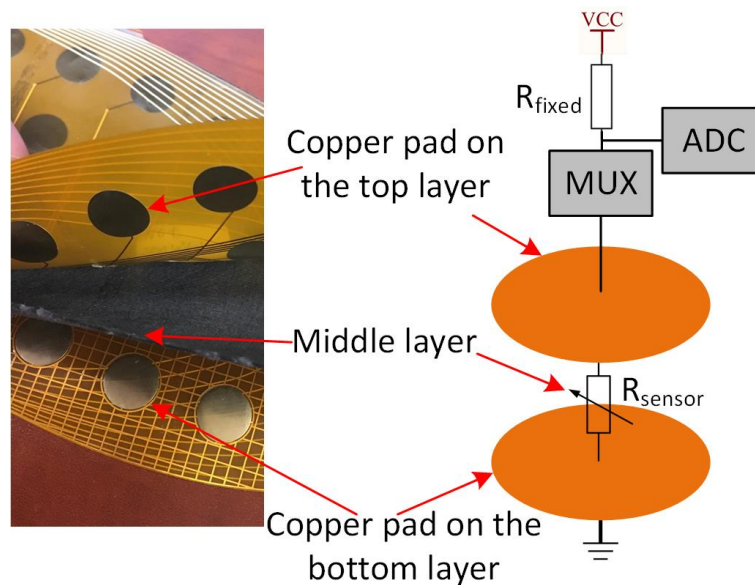
Figure 28: The structure of the robotic skin proposed by Chen D et al. © 2018 IEEE.

Google's Jacquard

A fabric microcomputer is connected to the Jacquard application. With gestures, touches, or a light change, it can play or pause music, display photographs and alerts, answer calls, and more. Jacquard yarns use conductive metal alloys combined with natural and synthetic fibers to create threads. They are connected and sewn from industrial looms used with natural fibers.

LifeChair from the University of to Tsukuba

This application is a "smart" pillow with sensors based on conductive fabric. Its purpose is to inform the user when their sitting posture is incorrect, using sensors to detect the posture and vibrations for alerts to the user.

The Atmega328 processor of the cushion houses the sensing, motor, power and communication modules. Its nine circular fabric sensors are made of nickel, copper, and polyester. The materials are sewn to the fabric and supported by acrylic glue. The cables required for the system are welded to a copper strip on the sensors and connected to a multiplexer. Next to this layer of sensors there is a conductive polyethylene film filled with carbon, providing insulation and electrical resistance to

the system. The last layer of conductive fabric comes in direct contact with the user and transmit signals to the other layers. [82]
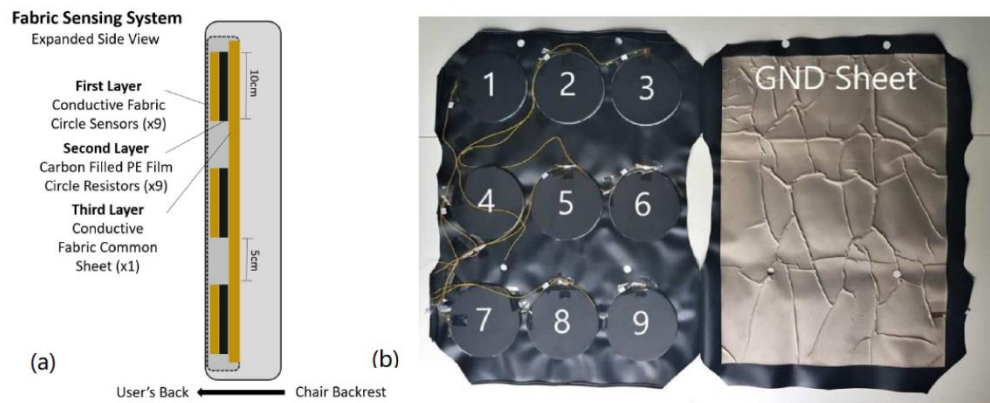
Figure 29: Presentation of LifeChair layers. (a) Description of the materials in the pressure system. (b) The sensing system made of conductive textiles and conductive film. © 2018 National Center for Biotechnology Information, U.S. National Library of Medicine.

3.6 The technology of flexible printed circuits

To meet modern technological needs in areas such as the health industry, the small size of the circuits is favored. This scale is achieved thanks to the modern construction methods such as 3D printers. Flexible printed circuits have high scalability. Micromechanics, even nanomechanics, is expected to become more easily accessible in the future.

Ultra-small circuits are printed with photolithography, electrical ink and graphene on paper, plastic film or some other flexible material such ionic gel. Memories, transistors, sensors, and LEDs can be part of the general circuit. This is the "active part", which is placed between layers of conductive and non-conductive materials. These layers contribute to the smooth operation and mechanical stability.

The safety of the mechanical parts within these structures must be noted. The polymeric plastic films used for casing are impermeable to water, oxygen, carbon dioxide and other materials and can withstand very high temperatures. Some parts of circuits, such as memory, can also be made of organic materials. [83]

The materials and methods chosen can be environmentally friendly. These include chemical-free printing techniques and memories and transistors made of organic materials. Low cost is also easily achievable.

When a device is printed on elastic substrates, its electrical properties may degrade over time due to the porous surface of the substrate. However, this can be solved with techniques such as stacking graphene in multiple layers. [84]

This technology is becoming increasingly popular due to the high performance of these circuits and the environments in which they can be integrated. At the moment, they can be embedded on of clothes and smart electronics and can join the Internet of Things (IoT). An example is the Akida microchip from the brainchip company, which operates as an integrated accelerator or as a co-processor with 1.2 million neurons and 10 billion synapses. It contains interfaces for IoT sensors, ADAS (advanced driver-assistance systems) sensors, audio sensors and more. Various devices can use it.
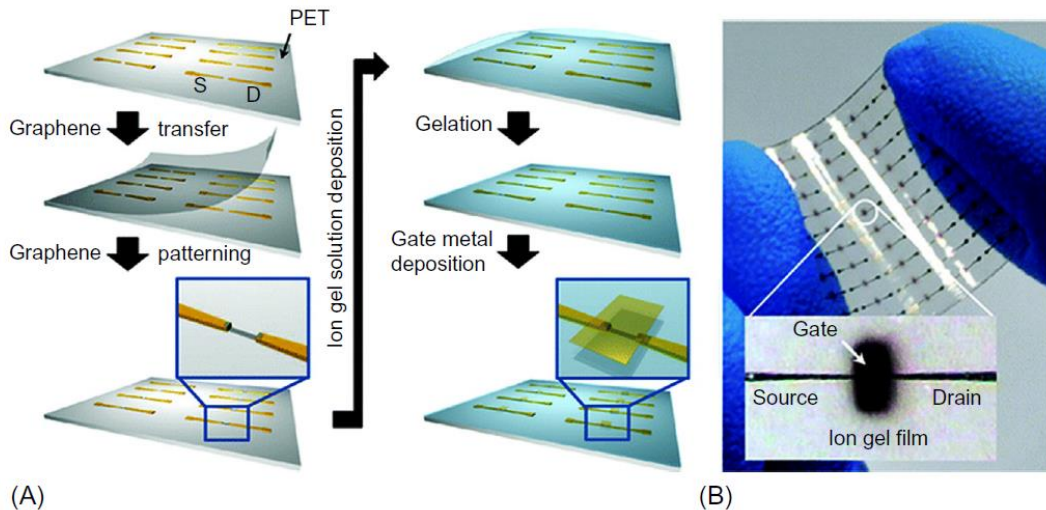
Figure 30: (A) Representation of a process of making a circuit from a transistor with graphene on plastic. (B) Picture of the actual circuit. © 2018 Elsevier Inc.

In the health sector, these circuits collect biological and behavioral data from patients when they are on their clothing but also on their internal organs. This way sensors, optoelectronic systems and more communicate with the patient's body and substances can be delivered directly in the least invasive way. High accuracy is another advantage of those systems.

In experiments with living mice, a series of electrodes (iWEBS system) inserted into their skull sent the appropriate signals to correct symptoms in seizures. [84] Lee H et al. presented a sensor with a printed circuit which could detect the levels of glucose from the sweat on the skin of the user. [85] M. S. Mannoor et al. pioneered a wireless bacterial detector based on graphene which is embedded on the tooth enamel. The circuit in this application is printed with graphene on bioabsorbable silk. [86]
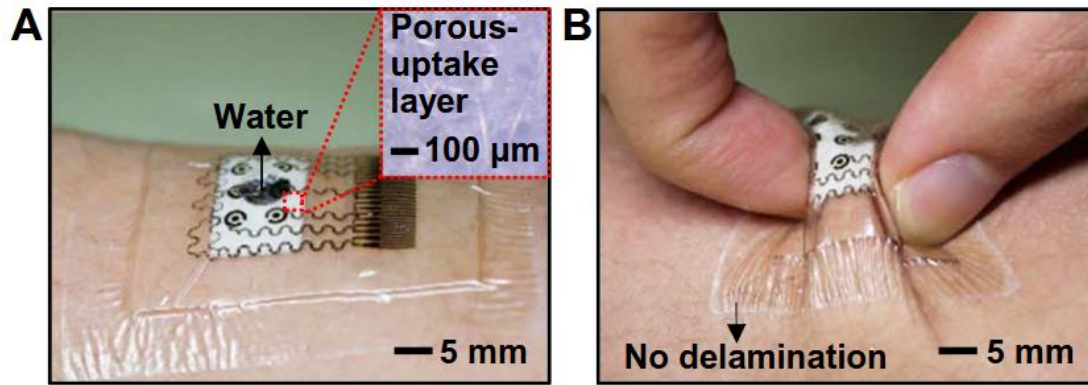
Figure 31: Sensor for detecting the amount of glucose from sweat. © 2017 National Center for Biotechnology Information, U.S. National Library of Medicine.
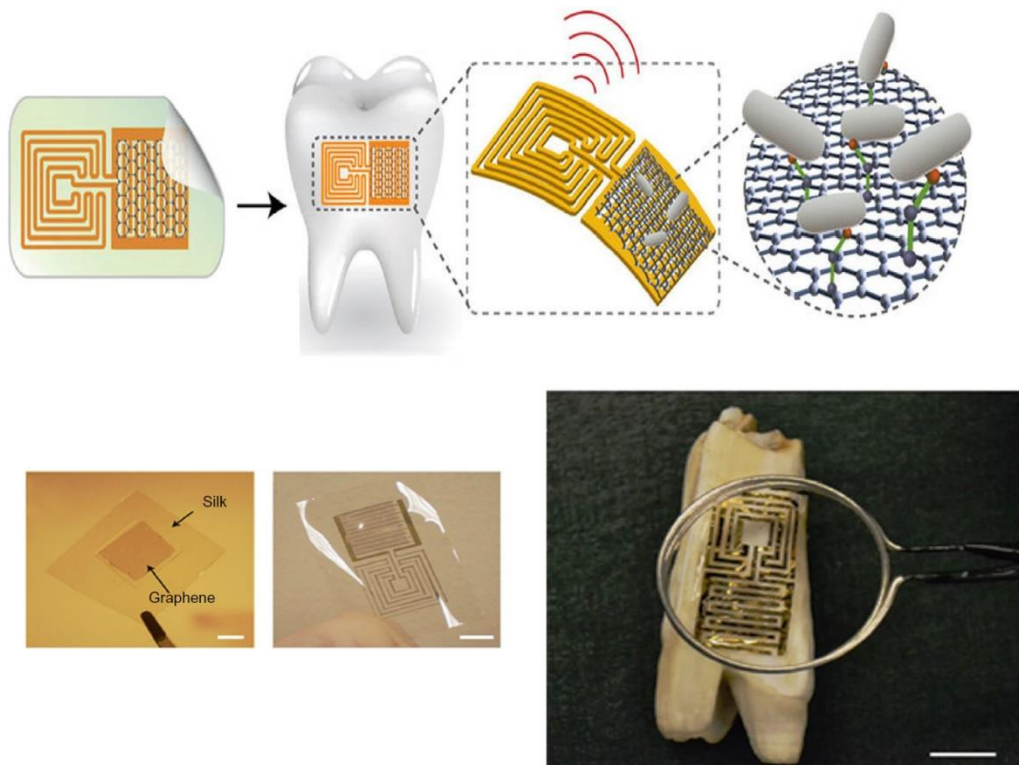
Figure 32: Wireless bacterial detector. © 2012 National Center for Biotechnology Information, U.S. National Library of Medicine.

Challenges have arisen from this new technology. Printing techniques may not have excellent performance due to the flexible nature of the surfaces hosting the circuits. In memory integration, depending on the construction method, there may be some problems. The most common are sparse integration of components, insufficient data transfer, lack of interconnection, unstable state of high resistance, and high-power consumption. Sometimes it is not possible to select a memory block. On harder membranes, complex memory microcircuits are difficult to implement.

However, it seems that with the right choice of materials and by taking into account the needs of the application, it is possible to build a nanometer-sized system of satisfactory performance.

4 System requirements

4.1 The necessity of documenting system requirements

Documenting system requirements is a way to analyze the problem that our application is called to solve.

From this analysis emerges a better understanding of the characteristics of the system and how each of them responds to the environment and the user. The accurate and simple description aims at an efficient implementation and further control of the operation of the system.

First, it is necessary to measure the needs that will be met by the system, and the environment in which it will replaced, before designing it. Next, the benefits of the system to the user must be defined and the operation process must be considered. Thus, possible undesirable effects and problems of the application come to our attention. The functional and environmental constraints are identified, as well as the most suitable ways of using the system.

The process leads to the confirmation or rejection of ideas for the system so that the final result meets the needs of the users as much as possible and adapts appropriately to the environment for which it is intended.

Table 2: Reviewed characteristics of the prototype

1. Sensing subsystem	2. Operating subsystem
A. Sensing System	
1. Touch	-
2. Force	-
B. Communication System	
1. Wires	1. Wires
C. Actuator system	
Stepper Motor moved rack	Stepper motor tugged thread
D. Information system	

4.2 The software quality standard ISO/IEC 9126

In an application run and controlled by computer programs, the employed software is just as important as the hardware. The software plays a key role in the development and operation of the application. Systems such as embedded systems, real-time systems and control systems can't function without it.

The basic principles of software quality assurance are the same as the quality assurance of any other product, but the production process is different. In the production of material goods, the specifications and characteristics of a prototype are first defined and then a series of products are manufactured, each being a replica of the other. In the case of software, the product is only created once and then exact copies of it are distributed.

The international standard ISO/IEC 9126 has been developed by the ISO Organisation (International Organization for Standarization) and the International Electrotechnical Commission (IEC) with a purpose to set global standards for technology. It is one of the most applied standards in the world for software evaluation. It is based on older ISO standards and various older standards such as ISO 9000 and McCall, Boehm, FURPS. [87]

This standard includes six main quality criteria which are divided into twenty-seven sub-criteria. The six major features are functionality, reliability, usability, efficiency, maintainability, and portability. For a software to be considered valid, it must comply with all these criteria.

Figure 33: The ISO/IEC 9126 standard and its six main features

Functionality is defined as the ability of a software product to provide and support functions that meet specified requirements under specific conditions. **Reliability** is the ability of the product to maintain a standard level of performance under specified conditions. The term **Usability** expresses how understandable and accessible the product is to the user. The ability of the product to produce results in an advantageous way compared to the volume of resources used under certain circumstances is called **Efficiency**. **Maintainability** describes the capacity of the product to be modified, i.e. to receive corrections and improvements in order to better integrate into the operation environment. **Portability** is the ability of a product to be transferred from one software environment to another. [87]

Table 3: The main criteria and the sub-criteria of the standard ISO/IEC 9126

Functionality	Reliability	Usability
Suitability	Maturity	Understandability
Accurateness	Fault Tolerance	Learnability
Interoperability	Recoverability	Operability
Security		Attractiveness
Efficiency	**Maintainability**	**Portability**
Time Behavior	Analysabilty	Adaptability
Resource Utilization	Changeability	Installability
	Stability	Coexistence
	Testability	Replaceability

4.3 Requirement Categorization

4.3.1 User Requirements (U.R.)

They describe in simple and natural language the services provided by the system, as well as its operational limitations. In our under-design system these are:

U.R.1.   A control system similar to those already existing surgical robots.
U.R.2.   Touch feedback available.
U.R.3.   Force feedback available.
U.R.4.   Interaction of the user with the system.
U.R.5   Interaction of the system with the user.
U.R.6.   Usableness of the System.

4.3.2 System Requirements (S.R.)

These describe what needs to be implemented:

S.R.1.   Attachment of the sensors to the internal side of the graspers at the end of their robotic hands.
S.R.2.   Attachment of the actuators on its control console.
S.R.3.   Achievement of low cost.
S.R.4.   Small volume system.
S.R.5.   Sensor based on conductive fabric.
S.R.6.   Stimulus feedback to the operator via the console.
S.R.7.   Microcontroller programming with memory integration.
S.R.8.   Wired data transfer.
S.R.9.   The power supply does not affect the operation of the robotic system.

4.3.3. Operational Requirements (O.R.)

They describe exactly what the system functions do. In our under-design system, these are:

O.R.1.   Measurement of natural values (touch, force).
O.R.2.   Operation in a surgical environment.
O.R.3.   Data input from a sensor adapted to a robotic mechanism.
O.R.4.   Output in tactile form on the control console (touch, force).
O.R.5.   Material texture categorization based on sensor capacity.
O.R.6.   Categorization of applied force based on the capacity of the sensor.
O.R.7.   Activation of actuator based on sensor input.
O.R.8.   Feedback adjustment based on configurable mechanism.
O.R.9.   Identification of organic / inorganic material.
O.R.10. Force reduction by the robotic system.

4.3.5. Non-functional Requirements (N.F.R.)

They accurately describe the limitations of the system functions. For our system they are the following:

N.F.R.1.   Placement in a surgical environment.
N.F.R.2.   Sensor resistance to disinfection.
N.F.R.3.   Activator resistance to disinfection.
N.F.R.4.   Biocompatible sensor casing.
N.F.R.5.   Time sampling per 1".
N.F.R.6.   No data retention required.
N.F.R.7.   Accuracy of force measurements.
N.F.R.8.   Utilization the microcontroller.
N.F.R.9.   Attachment of the system to different robots with minor modifications.
N.F.R.10.   Ability of operation on different computer operating systems (MS Windows, Mac, GNU/Linux).
N.F.R.11.   Non-autonomous operation.
N.F.R.12.   System maintenance by changing components.

5 System design

5.1 Introduction

The system includes of two parts which operate independently but communicate with each other. The first is the Sensory Device (SD), the set of elements that receive stimuli from the environment. The latter is the Feedback Device (FD) which communicates the values to the user by haptic methods.

In this chapter the implementation of each subsystem separately is described, hardware and software. In the application was used only open-source software and hardware.

5.2 Hardware development platform

The SD and the FD were built by using specialized hardware, more specifically the Arduino Mega 2560 Rev3 board. It is based on the microcontroller ATmega2560. Its numerous pins (54 digital input/output, of which 15 can be used as PWM outputs) were suitable for the complexity of our project. It was also chosen due to its small size and low power consumption, as well as its programming capabilities, the availability of an operating system and the support of endogenous (built-in) communication protocols and shield integration.

Figure 34: The Arduino Uno R3 board. © 2021 Karlsson Robotics.

On the Arduino Mega 2560 Rev3 board we mounted a Motor Control Module (or Motor Control "Shield") by Waveshare. Because of its dual H-bridge driver chip D, it can drive two stepper motors at the same time.

Figure 35: The Motor Control Module. © 2021 Waveshare Electronics.

5.3 The Sensory Device

There is a capacity sensor made of conductive fabric (S1), designed for embedding in the internal part of the surgical tool integrated at the end of the robotic arm. It detects the force applied by the robotic arm on the patient, as well as the texture of the organic and inorganic elements in the patient's body.

To differentiate between the values of touch and force that will be visualized to the user, the system will calculate force when there will be pressure from the console to the forceps, and touch where there will be no pressure. The existence of pressure will be measured by the distance of the two finger handles at any given moment. The displacement is calculated with a linear stretch sensor (S2) mounted on the controller.

The SD is wired to the FD and the FD responds according to the values the SD receives.

5.3.1 Capacitive Fabric Sensor

A voltage detection sensor based on conductive fabric was implemented, using two digital pins and a resistor. The conductive fabric together with the element it comes in contact with act like the two surfaces of a capacitor.

Figure 36: The conductive fabric used. © 2021 Hellas Digital.
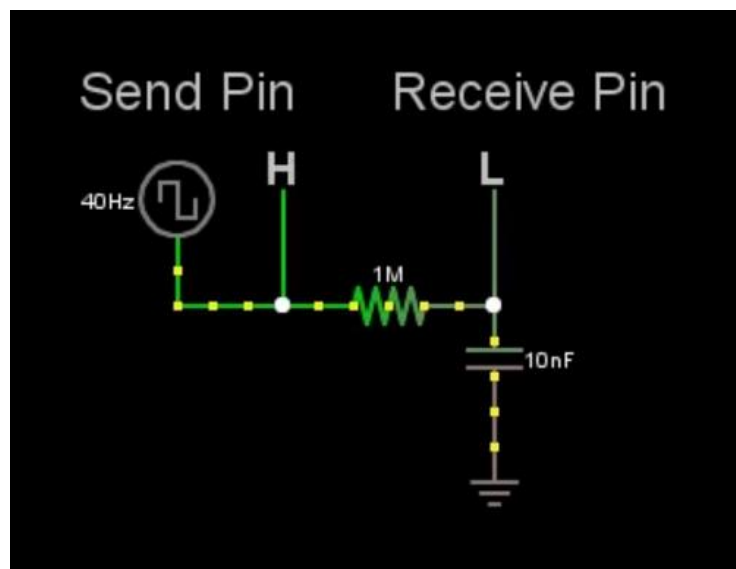
Figure 37: The sensor circuit as shown in Circuit Simulator.

The sensory area is a conductive knitted fabric with a silver coating. It is extremely conductive, made to have a resistance of less than 1 ohm per foot (0.3 m) in any

direction across the fabric. The silver coating was chosen due to its antibacterial properties. [76] Fungi, microorganisms, and even many viruses cannot grow on it. It also has low cytotoxicity to biological cells. [88], [89], [90]

Fabric 2 cm in width and 8.5 cm in length was utilized. The sensory area was 4.5 cm long as the rest of the space was used to place cables and fasten it to a thin piece of wood and then to plastic.

The sensor is intended for placement in the internal surface of a surgical forceps, suitable for laparoscopic surgery. Such tools with a diameter of 3mm, 3.5mm or 5mm and a length of 15mm are currently on the market. To cover these dimensions, an alternatively 5mm wide and 25mm long fabric was tested. The sensory area is then 5mm in diameter and 15mm long.

5.3.2 Rubber Stretch Sensor

The pressure the surgeon will exert on the patient's body can be measured by how tight the forceps will close. As this is directly connected to the movement in the handle, we can have an impression of the force by calculating the distance between the rings of the index and the thumb fingers.

For that we used conductive rubber cord made of black rubber with integrated conductive carbon particles. It's 2mm in diameter, and its resistance is 140 - 160 ohms per centimetre. It can be extended at 50-70% longer than its resting length. The material is used for the protection of sensitive electronic so it will also be guarded against electromagnetic interference. It has also entered the wearble electronics industry, since it can be incorporated into fabric.

Figure 38: The components for the stress sensor. © 2021 Grobotronics.

We used ten centimetres, with the active area being four centimetres. We attached one side of the chord to the index handle and the other to the thumb handle with alligator clips. The conductivity decreases linearly as the material gets stretched. The component is durable and stretchable enough for our application and it can operate in 5V. Moreover, it only requires three pins from the Arduino, in order to be connected to a voltage divider circuit.

The bigger the stretch the higher the values it sends to the microcontroller.

5.3.3 Processes flow and Assembly

The connections were made on a breadboard, as shown in the schematic diagram below. The power supply was chosen to be 5V as it is the common operating voltage level of the sensors and the feedback system on the operator console. The following figure describes the flow of process in the system.
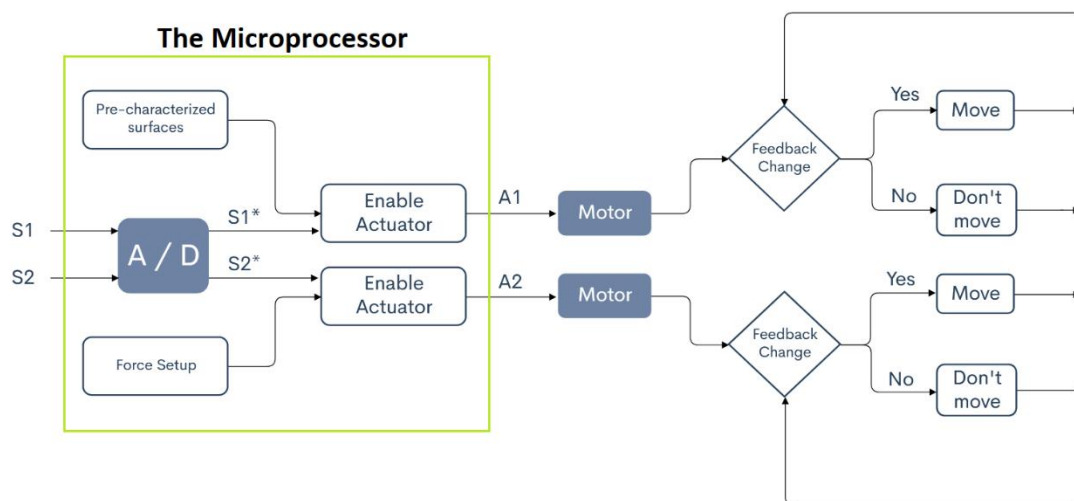
Figure 39: The Process Flow

The blue nodes show the hardware parts of the system, whereas the white show the software ones. The fragment of the flow which is included in the green area is the microcontroller.

The fabric capacitive sensor of the forceps is called S1 and stretch sensor between the two finger rings of the console is called S2. The sensors provide the system with analog signals which first go through an analog-to-digital converter. The now digital signals enable one actuator each. The two motors are responsible for moving the plastic components, from which the surgeon will receive tactile feedback. The A1 is the "surface actuator" (A1) and A2 is the "force actuator".

For each actuator to be enabled, values have to be collected from the environment. How the specified values will be processed and what outcome they will produce is

written in the code for Arduino, as we show in chapter 6. The "pre-characterized surfaces" refer to the levels defined by the capacitive sensor's ability to detect the textures of different objects during the testing process. The "force setup" is a similar table with the levels that have resulted from the stretching of the stretch sensor during testing.
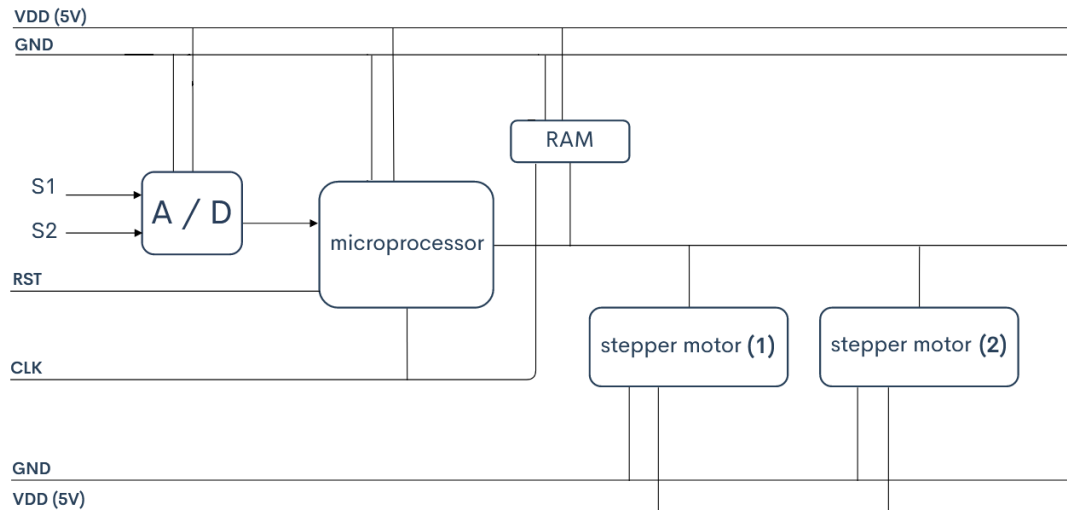
Figure 40: Architecture Layout
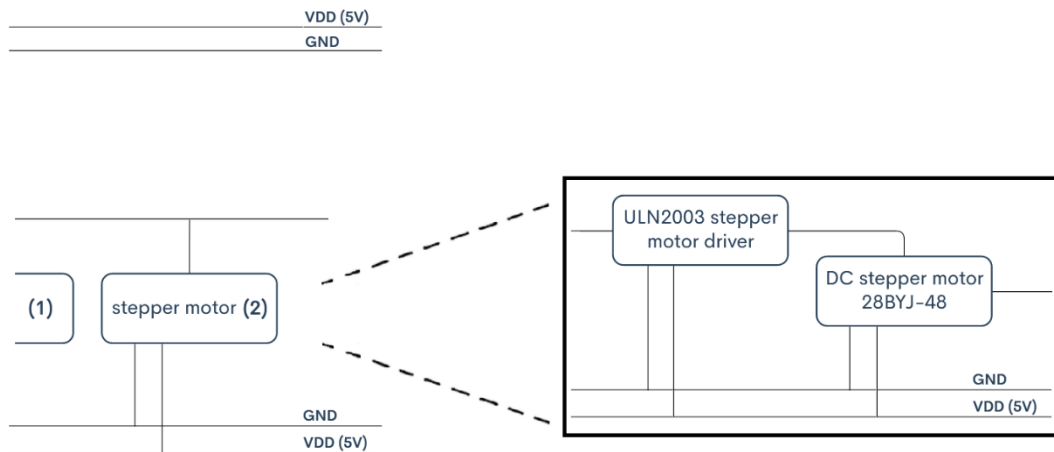
Figure 41: Continuation of the Architecture layout, focusing on the motor mechanism.

The signals from the sensor enter the converter and later the microprocessor, which shares Reset and Clock with the RAM of the Arduino board. The signal later passes to the two motors through the driver mounted on the board. In the memo below the properties of the architecture are described.

Table 4: Memo of Figure 38

Component	Details
Microprocessor	Arduino Mega 2560 Rev3
A/D	10 bit
RAM	8 kb
Stepper Motor	DC stepper motor 28BYJ-48
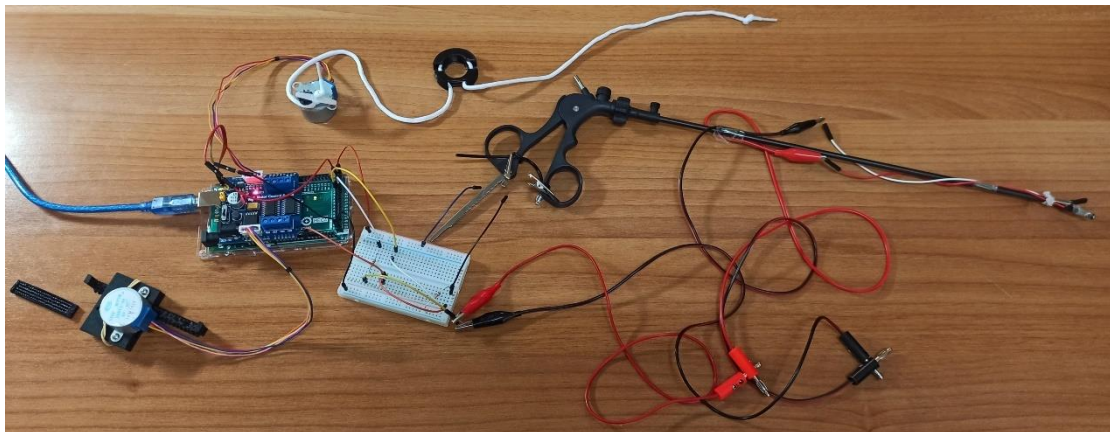
Figure 42: Proof of concept

In **Figure 43** all the sensors, actuators, boards, and parts have been assembled. The software has been uploaded to the Arduino Mega board on the left. Above the board stands the motor controlling the thread which tightens and loosens the plastic ring, in response to the stress in the stretch sensor. To the far left the other motor moves the rack with the rugged surface on its tip, after the evaluation of the fabric sensor.

Both sensors are mounted on the laparoscopic forceps to the right. The stretch sensor is shown tied between the two finger handles and connected to wires through crocodile clips. The scissor-like handles are the closest to the real-life console the surgeon operates.

Figure 43: The console of a robot assisting in laparoscopic surgery. © 2021 Intuitive Surgical, Inc.

In our application a tiny piece of conductive fabric has been secured onto the metallic grip of the surgical instrument. The metallic surface doesn't interfere with the input signal, since we separated it from it with insulating tape. The wires must be lengthy to transfer the signal from the fabric sensor to the board.

They are fastened on the long shaft, so as not to weigh down the forceps on the tip. Even thinner and longer wires can be used and it will be possible for the instrument to pass through the small incision in the patient's body.

5.3.4 Code

The programming of both system devices was done in the Arduino microcontroller development environment. The code is listed in Annex A.

The free open-source library `CapacitiveSensor.h`, created by Paul Bagder and Paul Stoffregen, was inserted. It directs input and output through registers and bitmask as found in OneWire library. In our application it converts the conductive material between two or more Arduino pins into a sensor that detects electrical potential in the human body. In this case we used two digital pins, 30 and 31. Only one value is returned, the potential difference between pins 30 and 31. In the code smoothing is happening for every ten values for the better visualization of the data.

We also utilized the library `<Motor.h>`, as it allows the operation unipolar or bipolar stepper motors. It works alongside the library `<DEV_Config.h>`, which provides the hardware with the configuration needed for the integration of the motors on the Arduino board. `<DEV_Config.h>` defines the pins, as well as the basic functions of the motors, such as digital initialization and exit, the delays, establishing the communication method, and digital write and read. `<Motor.h>` and `<DEV_Config.h>` are accompanied by .cpp files of the same names.

In our code, a capacitive sensor is declared with `CapacitiveSensor cs_4_2 = CapacitiveSensor(31,30).` For the smoothing of its values we insert 30 samples into the `current_read,` by writing `current_read = cs_4_2.capacitiveSensor(30).` The Smoothing algorithm reads repeatedly from an analog input, calculating a running average of the ten readings in the array, which changes dynamically.

With `Motor_Init(MOTOR_DEV_1, MOTOR_DEV_2)` we set up the two motors in our system. Moreover, the readings and averages are initialized to zero. We define an average and the previous average for touch and force values respectively, as well as the limits of value levels. In a series of else-if statements we check if the values fall into certain levels, which were generated during the experimental process.

If the current value belongs to the same level as the previous one, the motor stays in idle condition. If the level changes, the motor is prompted to turn accordingly. Different degrees and directions have been defined depending on the configuration and the motor. The values from the Rubber Stretch Sensor trigger Motor 1 and the values of Capacitive Fabric Sensor trigger Motor 2. Motor 1 turns in wider angles, whereas the changes in the Touch mechanism caused by Motor 2 are more subtle.

5.4 Feedback Device

It is designed to be embedded on the console of the robot. It consists of two parts, the force feedback (FF) and touch feedback (TF). They were designed on Tinkercad and printed by a 3D printer. The user will be notified with sensory stimuli to their fingers. Both parts will be connected to the two finger handles of the console.

Our application makes sure to prevent overwhelming the operator with stimuli. The user won't have to actively pay attention to indications on the screen, but information will be transferred through natural means through tactile feedback. Information from sense is processed more organically. With some training the process will become a natural part of the procedure.

5.4.1 Force Feedback

For the FF was designed and printed by a 3D printer a plastic ring that narrows around the user's finger in proportion to the pressure it will exert. The contraction of the ring is done with a cord wrapped on its interior. One end of the cord will remain fixed relative to the position of the ring and the other will be pulled or loosened by a small 5V DC stepper motor 28BYJ-48. The plastic ring will also have a stable position relative to the handles in the console, so as to provide a secure position for the finger.
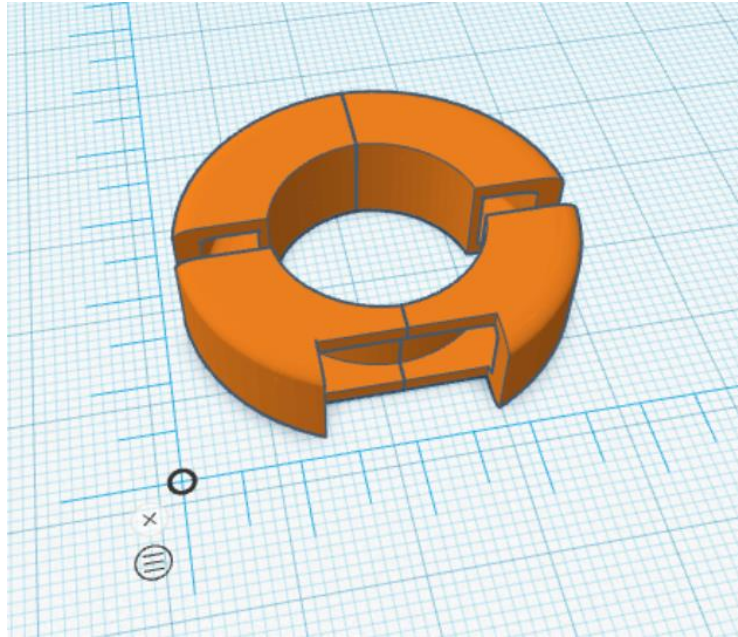
Figure 44: The Tinkercad design of the plastic ring. © 2021 Autodesk, Inc.

It encircles the thumb of the user. The parameters of the software have been defined so as not to press too tightly on the skin or cut circulation at the crucial time of the surgery.

5.4.2 Touch Feedback

For the Touch Feedback a surface has been designed to rest on one of the user's fingers. A plastic rugged surface about half the width and length of a finger gives feedback to the user. It is attached to the ring handle of the forceps and the red surface protrudes through the blue, which remains static. The higher the values received from the SD, the more this surface is pushed up and the more intense the stimulus is for the user.
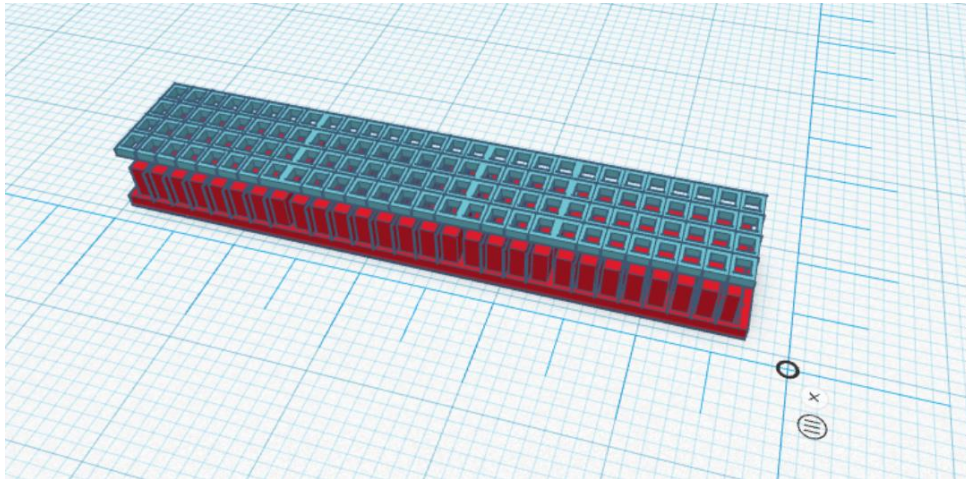
Figure 45: The Tinkercad design of the sliding surface. © 2021 Autodesk, Inc.

This component is attached to the end of a plastic but sturdy spur rack. In the mechanism shown in **Figure 46**, a stepper motor is placed downside and it's turning end is integrated into a gear. This gear then is attached to the spur rack. When the motor runs, the rack will be moved forwards or backwards depending on the angle and direction of the turn. This free open source design was collected and printed on a 3D printer for our project.
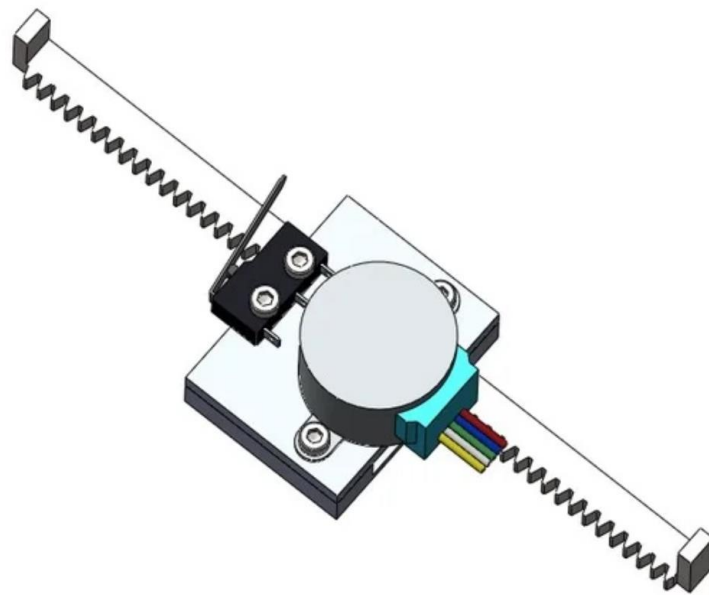
Figure 46: Design of a linear actuator for byj48 stepper motor, made by Tucker Shannon. © 2021 MakerBot Industries, LLC

6 System Evaluation

It is necessary to set levels of values that will determine the output to the operator. Output values will relate to touch and pressure on organs and other targets in the patient's body. The touch sensor is able of detecting pressure as well, but, because there could be confusion as to whether it shows sense or force, force values will be received from the stretch sensor.

The feedback from the fabric sensor will be interpreted better with the integration of the stretch sensor. The system response is transferred to the user in through nine (9) haptic configurations. Those are combinations of the levels of Touch and Force the user will receive in real time. Only one configuration will be felt by the operator for a predefined timespan. These configurations are:

1. Smooth Texture – Light Force
2. Smooth Texture – Intermediate Force
3. Smooth Texture – Strong Force
4. Intermediate Texture – Light Force
5. Intermediate Texture – Intermediate Force
6. Intermediate Texture – Strong Force
7. Rough Texture – Light Force
8. Rough Texture – Intermediate Force
9. Rough Texture – Strong Force

To collect values, the stretch sensor was tested and a variety of objects with different properties were came in contact with the fabric sensor in order to record their effect. Organic elements were used to simulate the texture of biological organs. The results were then categorized into three large groups, which will be responsible respectively for the configurations of the stimuli the operator receives.

The tests were performed on a fabric 2 cm wide and 8.5 cm long, with the sensory area being 4.5 cm long. Tests were also performed on the smallest piece of fabric with a width of 5 mm and a length of 15 mm.

Once a smaller piece of fabric was embedded onto surgical graspers having an even more reduced sensing area and a similar response to the different objects was observed.

The conductive fabric is covered with transparent plastic wrap which is safe for contact with the organism at body temperature. The purpose was not to put the fabric in direct contact with the objects when examining their surface. The cover prevents any liquids from touching the fabric and protects its structure. The plastic is quite insulating and thin, allowing the reception of values from the environment.

To simulate a smooth surface on which objects would slide more easily, an adhesive tape was glued over the plastic wrap. Tests were performed with and without the adhesive tape with the results being proportionally different. Thus, we concluded that keeping the wrap wouldn't negatively affect the haptic feedback.

Each item tested had a different size and surface, so the collection of values may have lasted some seconds longer on some. However, it is certain that all possible values that may arise during the contact with a certain item are presented.

The materials selected for the test were organic, partly organic and inorganic. The organic materials are: wrapped minced meat, bone, skin (finger), liver in thin plastic wrap, cotton, tomato (whole), orange (whole), and dried fig. The partly organic items are: smooth seashell, rough seashell. The inorganic materials are: smooth stone, rough stone, smooth glass, smooth metal, rough metal (file), smooth plastic, rough plastic, rubber (eraser), rubber (filled ball).

The objects were moved by hand. The presence of the fingers has little effect on the prices compared to the movement with plastic forceps. The finger was preferred in the experimentation part since even in operating conditions there will be other organic elements around the target object.

The pressure exerted by all objects was the same for the same in a predefined timespan. We attempted to separate the pressure measurement from the texture as much as possible. So, the sliding was done with almost no pressure, whereas force was applied without any slipping of the object.

In real conditions, that is operating room conditions, what we are interested in is the organic elements. However, individual organic and inorganic objects were tested to see the response of the sensor in them as well. The results from the organic and inorganic materials provided indications for the overall operation of the sensor.

Finally, we examined whether the values from the sensor are reflecting the human sense. Something that will be evaluated as "compact" by humans, ideally should be evaluated as "compact" by the sensor. For this reason, organic materials were first categorized in ascending order in terms of human sense. Some items listed in the roughness category don't exist in the density category, since the sense of an item is the same, no matter its size.

Table 5: Categorization of organic material roughness based on human sense.

"SMOOTH TEXTURE" CATEGORY
cotton
liver
tomato (whole)
"INTERMEDIATE TEXTURE" CATEGORY
wrapped minced meat
skin (finger)
bone
"ROUGH TEXTURE" CATEGORY
orange (whole)
dried fig

Table 6: Categorization of material density based on human sense.

"WEAK CONSISTENCY" CATEGORY
cotton
orange peel
dried fig
tomato peel (with flesh)
"INTERMEDIATE CONSISTENCY" CATEGORY
tomato (small mass)
bone
wrapped minced meat (small mass)
skin (finger)
"STRONG CONSISTENCY" CATEGORY
tomato (whole)
orange (whole)
liver
wrapped minced meat (big mass)

6.1 Results from the Capacitive Sensor

It was observed that with or without the adhesive tape over the plastic wrap the values did not change.

The smaller piece of fabric gave proportionally similar prices to the larger one and followed the same principles, but its values were higher. The circuit remained the same and its resistance did not change. It is natural for higher values to appear. The values are determined by the current voltage created between the two ends of the piece of fabric. The larger its surface, the smaller the voltage between its edges, since the fabric itself has a small resistance.

To explain this, we can consider the conductive fabric as a wire. In circuits, the larger the cable, the greater its internal resistance. In the smaller wire, however, we have minimal resistance compared to the large one, so more current will flow through it at any given time compared to the larger one.

This happens as long as the resistance of the circuit stays unaltered. According to Ohm's law, when the current increases, the voltage increases proportionally. For this reason, on the smaller surface, where more current passes through each time, we have a higher voltage, which results to higher values. If we properly increase the circuit's resistance the values from the smallest part will be in the same range as the largest.

More importance was given to the tests with the largest piece of fabric and these will be presented below. Whether the values were presented from the large or from the small size, the response of the sensor would be the same. In addition, the small size is not binding. The fabric can be placed in smaller graspers, or cut for a slightly larger one. In any case, the parameters that apply to the large piece will be implemented.

6.1.1 Touch

The organic objects gave the highest values overall. As shown in **Figure 48**, the skin, bone, liver, dried fig, tomato, orange and minced meat stimulated the sensor the most. It seems that the sensor gives higher values to the roughest, but also to the materials with the largest amount of water. This is why it sometimes the liver gives higher values than the rougher dried fig. On the other hand, the roughest organic items gave higher values than the smoother organic ones.

Even in the hardest and heaviest materials the values were relatively low if their surface was smooth. Therefore, weight was of no consequence. Where possible, a smooth and a rough item of the same material were tested (for example, smooth metal and rough metal, smooth seashell and rough seashell).

The inorganic items gave the lowest values of all. Rough objects gave slightly higher prices than the smooth ones when the material was the same.

The values for the partly organic items, meaning the smooth and rough seashells, ranked somewhere between inorganic and organic objects, slightly above the prices of the inorganic ones. The smooth seashell surpassed almost all the inorganic items but was still below the rough seashell.

Compared to the human sense, the values were categorized similarly, with small differentiations.

The three items with the highest values were the liver, the dried fig and the orange. For the dried fig and the orange, the results were expected, but the liver had been classified as smooth by human touch. The bone was, for the most part, in the Intermediate level, as had been categorized by human touch, but for its valued touched the Rough Texture level, as well.

The following categorization of organic items is based on the maximum values the sensor received from each one.

Table 7: Touch values from the sensor

"SMOOTH TEXTURE" CATEGORY
cotton (40)
"INTERMEDIATE TEXTURE" CATEGORY
tomato (143)
wrapped minced meat (143)
"ROUGH TEXTURE" CATEGORY
bone (160)
Skin (finger) (185)
orange (187)
dried fig (196)
liver (285)
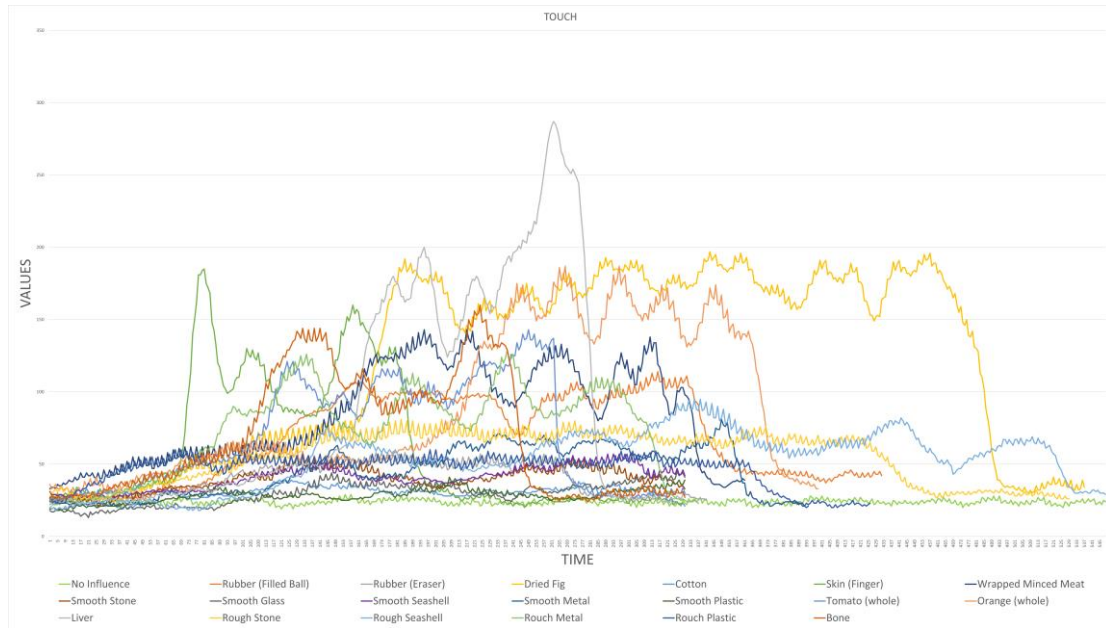
Figure 47: A diagram of the Touch values taken from the sensor

6.1.2 Force

As in the Touch values, we receive higher values from the sensor when the items are organic and especially when they contain a large amount of water. There are sharp changes in the values of rough objects, which is to be expected since the surface of those objects is irregular and does not always touch the fabric in the same way.

The tests were performed with the sensor placed horizontally and vertically in relation to the ground, in order for us to investigate whether gravity plays a role in detecting pressure. It was concluded that the values do not change at different positions as long as the sensor is set in the same way.

Table 8: Force values from the sensor

"WEAK CONSISTENCY" CATEGORY
cotton (238)
dried fig (325)
"INTERMEDIATE CONSISTENCY" CATEGORY
orange peel (560)
orange (whole) (614)
bone (641)
tomato peel (with flesh) (646)
tomato (small mass) (728)
wrapped minced meat (small mass) (730)
skin (finger) (740)
"STRONG CONSISTENCY" CATEGORY
tomato (whole) (1117)
liver (1397)
wrapped minced meat (big mass) (1509)
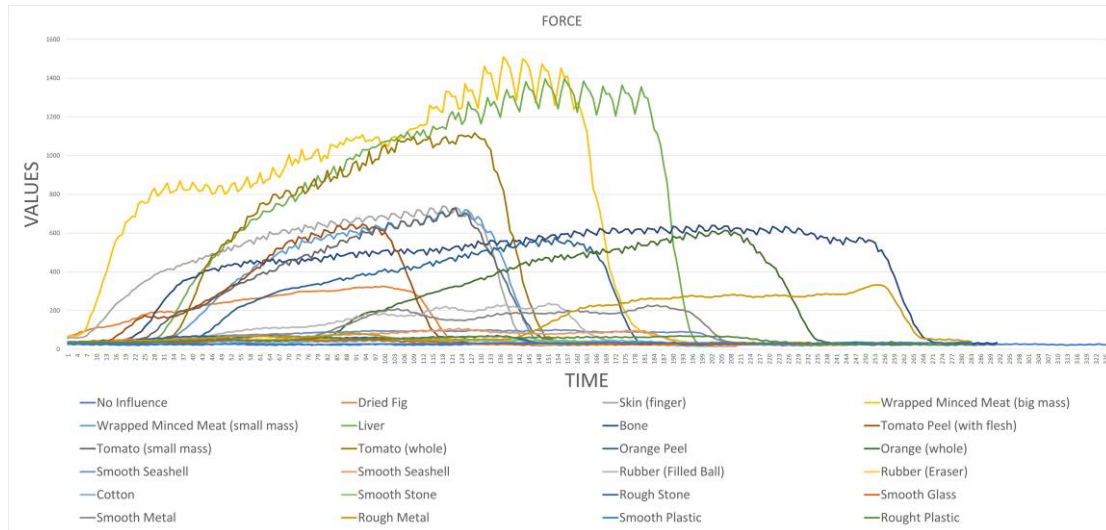
Figure 48: A diagram of the Force values taken from the sensor

The item "tomato (whole)" gave bigger values than "tomato (small mass)", which, in turn, gave bigger values than "tomato peel (with flesh)". Similarly, "orange (whole)" ranked higher than "orange peel", even though their sizes were close. Respectively, the "wrapped minced meat (big mass)" showed higher values than "wrapped minced meat (small mass)", albeit both items being from the same material.

It's important to note that the deviation in values between different masses of the same organic material became proportionally more significant with how thin the separator between the material and the sensor was. In the case of a thinner separator, such as the tomato peel and the plastic wrap around the minced meat, there were large divergencies. In surgery this could be translated into the fact that the organs with the thinnest walls will show increased force values. This can help the surgeon detect if the walls of an organ have thickened or hardened because of illness or injury and make a comparison with their healthy condition.

This deviation was also observed even in the inorganic materials. The items "Rubber (Filled Ball)" gave higher values than "Rubber (Eraser)" because the latter had smaller mass, despite both being similar to the touch.

An important factor was the density, i.e. the coherence of the molecules of an object. Water content also played an important role.

The existence of higher values recorded in organic objects, both in Touch and Force, works to the benefit of our application. This provides a wider range of feedback and allows us to better identify the elements that interest us, for example, the various tissues that are found in the body.

6.1.3 Grouping values

For Touch there are three categories for "Smooth", "Intermediate" and "Rough" texture, and for Force three more, "Weak", "Intermediate" and "Strong" consistency. Every category covers a range of values. As previously stated, an object can give values that belong to more than one category. However, it is important for the operator to know at all times which object or surface they are in contact with.

Table 9: The levels of Touch

VALUES	CATEGORY
0-100	"SMOOTH TEXTURE"
101-150	"INTERMEDIATE TEXTURE"
>150	"ROUGH TEXTURE"

Table 10: The levels of Force

VALUES	CATEGORY
0-400	"WEAK CONSISTENCY"
401-800	"INTERMEDIATE CONSISTENCY"
>800	"STRONG CONSISTENCY"

6.1.4 Code

Inside the Motor.cpp file, where the pins are initialized, we configured the functions `void Motor_Trun(BYTE Motor_dev, unsigned long Angle, int dir)`

and `static void Motor_Setbit(struct MOTOR sMotor,BYTE Data)` to allow the motor to turn clockwise and counter-clockwise. For the clockwise movement we make the `dir` variable 1 and, for the counter-clockwise movement, 0.

In our main code we set up the motor which will be responsible for the movement of the Force Feedback device. In the function `void Motor_Trun(BYTE Motor_dev, unsigned long Angle, int dir)`, the `BYTE Motor_dev` holds the name of the Motor used and the variable `unsigned long Angle` holds the absolute value of the number of degrees for the motor turn.

This motor rotates a gear pushing the rack back and forth. The turn indicates the slight pushing from the rugged surface at the end of the rack on the user's finger. The changes in rotation degrees and direction depends on the if-else statements. The conditions are defined as the limits of the different levels, which have been defined during the experimental process.

The conditions are specifically designed for the mechanism moved by this stepper motor. When values are obtained from the Fabric Capacitive Sensor, the code enters if-else conditions to determine if and for how many degrees the motor will turn. Once more, the levels of intensity are three, the first being the lowest and the third the highest, numerically and qualitatively. The bigger the change of level, the bigger the turn of the motor will be.

If there is a change from level 2 to level 3, the rugged surface needs to come in contact with the operator's finger more intensely. The motor turns in order to push the rack towards the finger. For a bigger change the motor executes a wider turn, and for a reverse change, it turns the opposite direction.

6.2 Results from the Stretch Sensor

The values from the stretch sensor fluctuated less compared to the values from the fabric sensor. Consequently, each level has a smaller span. However, we made sure this covers the span of the hand movement on the handles. The bigger the stretch on the sensor, the bigger the value it sends to our system. As the bigger stretch denotes a loser grip on the forceps, so the software will send feedback to the operator that the force is stronger at that time.

Level one, and with bigger force, includes the values 920 – 929, the second level and intermediate in force, contains values 930 – 939, and the third and milder level ranges from 940 and up.

Table 11: The levels resulted from the testing of the stretch sensor

VALUES	CATEGORY
920-929	"STRONG FORCE"
930-939	"INTERMEDIATE FORCE"
>940	"LIGHT FORCE"

6.2.1 Code

The stress sensor is connected to the analog pin 8, so it's declared as follows: `int SensorPin = A8.` It's initialized to zero with `int sensorValue = 0` and later becomes the force average.

The cord inside the ring moves through a step motor, which turns at an angle proportional to the force applied.

The second stepper motor is identical to the first. It utilizes the same libraries as the first one, `<DEV_Config.h>` and `<Motor.h>`, with the same alterations in the function `void Motor_Trun` inside the Motor.cpp. The same configurations apply in the functions `void Motor_Trun (BYTE Motor_dev, unsigned long Angle, int dir)` and `static void Motor_Setbit (struct MOTOR sMotor,BYTE Data).` The `dir` variable is, again, 1 for a clockwise turn and 0 for a counter-clockwise one.

Motor 2 is set up like motor 1. When values are obtained from the stretch sensor, the code enters if-else conditions to determine if and for how many degrees the motor will turn.

There are three levels of intensity. The first one has the lower numerical values and the third the highest. However, the higher the value the less pressure the forceps

exercise while gripping. Therefore, when going from lower to higher values the ring around the operator's finger lessens.

For example, from level 1 to level 2, the stretch on the sensor has been reduced, and at the same time the pressure from the forceps to the organ has been increased. To indicate that, the plastic ring tightens. So, the rope inside it needs to be pulled away from the handler. This is achieved with a turn 1/4 of a full circle. For a more drastic change, e.g. for level 1 to level 3, the ring needs to get tighter. Then, the motor turns 1/2 of a full circle. Those turns are reversed if there is a negative change in levels.

7 Conclusions and future work

7.1 Conclusions

In this thesis we were concerned about how robots that assist in minimally invasive surgery can be made more accessible to medical staff and patients. The advantages and disadvantages of robots in surgery were weighed, taking into account the surgeon and the operated patient.

The robots for surgery in the market were recorded and it was noted whether they provided the user with a sense of touch and applied force. It was observed that several offered values regarding force but none the sense of touch.

Having the above knowledge, we proposed a low-cost support mechanism that complements the feedback that already exists from these machines to the operator. We thought that this would help not only the surgical procedure, but possibly also the detection or observation of organ diseases through touch.

Topics related to touch and force were studied, the two senses we intended to offer to the robot operator. The concepts of triboelectricity and piezoelectricity were introduced as well as innovative methods and materials used in modern technology. Conductive fabrics and stress sensors were studied and how they are used to make sensory systems, especially in the health sector.

A sensor based on conductive fabric was selected to detect the characteristics of the surfaces and the pressures exerted by the surgical instrument on them. The fabric has a similar response in all its sizes, so it is suitable to be added to microscopic surgical instruments in laparoscopic surgery.

Organic, partly organic, and inorganic objects were slid and pressed on the sensor in order to record its reaction to various textures and pressure levels. The widest range of values was observed in organic materials, which makes the sensor suitable for use inside the body. The two ends of the stress sensor were attached to the handles, for the detection of the user's movements.

The values obtained from the sensors during testing were calibrated and sorted into categories. Three levels account to each sensor. In total, nine (9) configurations were created. These combinations of stimuli will convey the sense of touch and pressure to the operator.

The segments of the haptic feedback sub-systems include 3D printed components moved by actuators. More specifically, the index finger of the operator comes in contact with a plastic ring finger of adjustable size and their thumb with a thin rugged surface.

Free open-source hardware was used, and the software written by us and modified was free open source Arduino code. The program receives the values of touch and force, smoothens the touch values and triggers the actuators.

The application shows satisfactory performance, it is small in size and low in cost. The available materials seem to be able to meet the real-life operating conditions. Of course, we estimate that a slightly pricier implementation will take full advantage of the prospects of our prototype.

Our application will find better ground in the light of new discoveries in the field of electronics, such us the flexible micro / nano-circuits mentioned in chapter 3.6.

7.2 Future work

Our prototype is promising, but it can be made more efficient with additions and changes.

Building on a second data transmission option to the operating physician could be helpful. This method will transmit rates of increase in value in relation to values of the user's choosing and not those set by the manufacturer. In some cases, it may be more practical for the operator to receive a comparison to a previous value for a specific organ, or a comparison of values to an area close to it. This difference may not be high enough for change of level to be indicated but the operator may still want to know about it.

In terms of hardware, in the future the user feedback system should be properly integrated into a surgical robot control console and mounted onto the controller. For a seamless assimilation of the conductive sensor on the forceps we could stitch the conductive fabric onto a micro-sleeve of non-conductive fabric that will secure its position.

Later that sleeve can be covered with paraffin film, which makes the sensor waterproof, thus security from bodily and disinfection fluids. [64] It is also possible to use a thin polydimethylsiloxane dialectric elastomer surface (PDMS). This material has excellent elasticity when it's in contact with living cells and generally with human tissues. [91], [92] It will be a good separator between the fabric and the body environment and at the same time it will allow the sensor to receive signals from the tissues.

On the wiring we can use the latest fiber optic technology to prevent electricity leakage into the patient's body. Although the optical fibers do not bend as much as the metal wires, their elasticity is sufficient for our application. In addition, the system does not require much operating voltage, and this makes it suitable for optical fiber integration. [93]

ANNEX A

The libraries and files CapacitiveSensor.h , DEV_Config.cpp, DEV_Config.h , Motor.h and Motor.cpp belong to their respective owners and are presented as they were written. They are all in the public domain. Therefore, we are granted permission, free of charge, to deal in the Software without restriction, including without limitation, as well as the rights to use, copy, modify, merge, publish, distribute, and sublicense.

The public domain code of the smoothing algorithm was created by David A. Mellis and modified by Tom Igoe.

The Motor.cpp was modified by us as stated in Chapter 5.

Code

RoboticSubsystem.ino

```
#include <CapacitiveSensor.h>
#include "DEV_Config.h"
#include "Motor.h"


const int numReadings = 10;


int readings[numReadings];
int readIndex = 0;
int total = 0;
int avg_touch = 0;
int prev_avg_touch = 0;


int avg_force = 0;
int prev_avg_force = 0;


int SensorPin = A8;
int sensorValue = 0;


CapacitiveSensor   cs_4_2 = CapacitiveSensor(31,30);


int lvl_1_max_touch = 100;
int lvl_2_min_touch = 101;
```

```
int lvl_2_max_touch = 150;
int lvl_3_min_touch = 151;


int lvl_1_max_force = 929;
int lvl_2_min_force = 930;
int lvl_2_max_force = 939;
int lvl_3_min_force = 940;

void setup() {
   cs_4_2.set_CS_AutocaL_Millis(0xFFFFFFFF);
   Serial.begin(9600);

  for (int thisReading = 0; thisReading < numReadings; thisReading++) {
    readings[thisReading] = 0;
  }
      System_Init();

    Motor_Init(MOTOR_DEV_1, MOTOR_DEV_2);
 }


void loop() {

  int start = millis();
  int current_read =  cs_4_2.capacitiveSensor(30);
  sensorValue = analogRead(SensorPin);
  avg_force = sensorValue;

  total = total - readings[readIndex];
  readings[readIndex] = current_read;
  total = total + readings[readIndex];
  readIndex = readIndex + 1;

  if (readIndex >= numReadings) {
    readIndex = 0;
  }

  avg_touch = current_read; //total / numReadings;
  Serial.println(avg_touch);
  delay(10);

// force level 1 -> force level 2 . Turn 90 degrees counter-clockwise
```

```
    if (((avg_force >= lvl_2_min_force) && (avg_force <= lvl_2_max_force))
&& (prev_avg_force <= lvl_1_max_force))

{

    Motor_Trun(MOTOR_DEV_1, 90, 0);

    delay(1000);

    prev_avg_force = avg_force;

    }


// Force level 1 -> force level 3. Turn 180 degrees counter-clockwise


    else if ((avg_force >= lvl_3_min_force) && (prev_avg_force <=
lvl_1_max_force) {

    Motor_Trun(MOTOR_DEV_1, 180, 0);

    delay(1000);

    prev_avg_force = avg_force;

    }


    else if ((avg_force >= lvl_3_min_force) && ((prev_avg_force >=
lvl_2_min_force) && (prev_avg_force <= lvl_2_max_force)))

{

    Motor_Trun(MOTOR_DEV_1, 90, 0);

    delay(1000);

    prev_avg_force = avg_force;

    }


// Force level 2 -> level 1 . Turn 90 degrees clockwise


    else if ( (avg_force <= lvl_1_max_force) && ((prev_avg_force >=
lvl_2_min_force) && (prev_avg_force <= lvl_2_max_force)) )

{

    Motor_Trun(MOTOR_DEV_1, 90, 1);

    delay(1000);

    prev_avg_force = avg_force;

    }


    else if (       ((avg_force >= lvl_2_min_force) && (avg_force <=
lvl_2_max_force)) && ((prev_avg_force >= lvl_3_min_force) ))

{

    Motor_Trun(MOTOR_DEV_1, 90, 1);

    delay(1000);

    prev_avg_force = avg_force;

    }


    else if ( (avg_force <= lvl_1_max_force) && (prev_avg_force >=
lvl_3_min_force) ) {
```

```
    Motor_Trun(MOTOR_DEV_1, 180, 1);

    delay(1000);

    prev_avg_force = avg_force;

  }


  else {

    delay(1000);

  }



if (((avg_touch >= lvl_2_min_touch) && (avg_touch <= lvl_2_max_touch)) &&
(prev_avg_touch <= lvl_1_max_touch))

{

    Motor_Trun(MOTOR_DEV_2, 10, 1);

    delay(1000);

    prev_avg_touch = avg_touch;

  }


  else if ((avg_touch >= lvl_3_min_touch) && (prev_avg_touch <=
lvl_1_max_touch))

{

    Motor_Trun(MOTOR_DEV_2, 20, 1);

     delay(1000);

    prev_avg_touch = avg_touch;

  }


  else if ((avg_touch >= lvl_3_min_touch) && ((prev_avg_touch >=
lvl_2_min_touch) && (prev_avg_touch <= lvl_2_max_touch)))

{

    Motor_Trun(MOTOR_DEV_2, 10, 1);

    delay(1000);

    prev_avg_touch = avg_touch;

  }


  else if ( (avg_touch <= lvl_1_max_touch) && ((prev_avg_touch >=
lvl_2_min_touch) && (prev_avg_touch <= lvl_2_max_touch)) )

{

    Motor_Trun(MOTOR_DEV_2, 10, 0);

    delay(1000);

    prev_avg_touch = avg_touch;

  }


  else if (      ((avg_touch >= lvl_2_min_touch) && (avg_touch <=
lvl_2_max_touch)) && ((prev_avg_touch >= lvl_3_min_touch) ))
```

```
{
      Motor_Trun(MOTOR_DEV_2, 10, 0);

      delay(1000);

      prev_avg_touch = avg_touch;

    }


    else  if  (  (avg_touch  <=  lvl_1_max_touch)  &&  (prev_avg_touch  >=
lvl_3_min_touch) )
{
      Motor_Trun(MOTOR_DEV_2, 20, 0);

      delay(1000);

      prev_avg_touch = avg_touch;

    }


    else {

      delay(1000);

    }
}
```

CapacitiveSensor.h

```
/*
 CapacitiveSense.h - Capacitive Sensing Library for Arduino / Wiring

 https://github.com/PaulStoffregen/CapacitiveSensor

 http://www.pjrc.com/teensy/td_libs_CapacitiveSensor.html

 http://playground.arduino.cc/Main/CapacitiveSensor

 Copyright (c) 2009 Paul Bagder

 Updates for other hardare by Paul Stoffregen, 2010-2016

 vim: set ts=4:


 Permission is hereby granted, free of charge, to any person obtaining a
copy of this software and associated documentation files (the "Software"),
to deal in the Software without restriction, including without limitation
the rights to use, copy, modify, merge, publish, distribute, sublicense,
and/or sell copies of the Software, and to permit persons to whom the
Software is furnished to do so, subject to the following conditions:

The above copyright notice and this permission notice shall be included in
all copies or substantial portions of the Software.


THE SOFTWARE IS PROVIDED "AS IS", WITHOUT WARRANTY OF ANY KIND, EXPRESS OR
IMPLIED, INCLUDING BUT NOT LIMITED TO THE WARRANTIES OF MERCHANTABILITY,
FITNESS FOR A PARTICULAR PURPOSE AND NONINFRINGEMENT. IN NO EVENT SHALL THE
AUTHORS OR COPYRIGHT HOLDERS BE LIABLE FOR ANY CLAIM, DAMAGES OR OTHER
LIABILITY, WHETHER IN AN ACTION OF CONTRACT, TORT OR OTHERWISE, ARISING
```

```
// ensure this library description is only included once
#ifndef CapacitiveSensor_h
#define CapacitiveSensor_h


#if ARDUINO >= 100
#include "Arduino.h"
#else
#include "WProgram.h"
#endif


// Direct I/O through registers and bitmask (from OneWire library)


#if defined(__AVR__)
#define PIN_TO_BASEREG(pin)
(portInputRegister(digitalPinToPort(pin)))
#define PIN_TO_BITMASK(pin)              (digitalPinToBitMask(pin))
#define IO_REG_TYPE uint8_t
#define DIRECT_READ(base, mask)          (((*(base)) & (mask)) ? 1 : 0)
#define DIRECT_MODE_INPUT(base, mask)    ((*((base)+1)) &= ~(mask),
(*((base)+2)) &= ~(mask))
#define DIRECT_MODE_OUTPUT(base, mask)   ((*((base)+1)) |= (mask))
#define DIRECT_WRITE_LOW(base, mask)     ((*((base)+2)) &= ~(mask))
#define DIRECT_WRITE_HIGH(base, mask)    ((*((base)+2)) |= (mask))


#elif defined(__MK20DX128__) || defined(__MK20DX256__) ||
defined(__MK66FX1M0__) || defined(__MK64FX512__)
#define PIN_TO_BASEREG(pin)              (portOutputRegister(pin))
#define PIN_TO_BITMASK(pin)              (1)
#define IO_REG_TYPE uint8_t
#define IO_REG_ASM
#define DIRECT_READ(base, mask)          (*((base)+512))
#define DIRECT_MODE_INPUT(base, mask)    (*((base)+640) = 0)
#define DIRECT_MODE_OUTPUT(base, mask)   (*((base)+640) = 1)
#define DIRECT_WRITE_LOW(base, mask)     (*((base)+256) = 1)
#define DIRECT_WRITE_HIGH(base, mask)    (*((base)+128) = 1)
```

```
#elif defined(__MKL26Z64__)
#define PIN_TO_BASEREG(pin)              (portOutputRegister(pin))
#define PIN_TO_BITMASK(pin)              (digitalPinToBitMask(pin))
#define IO_REG_TYPE uint8_t
#define IO_REG_ASM
#define DIRECT_READ(base, mask)          ((*((base)+16) & (mask)) ? 1 : 0)
#define DIRECT_MODE_INPUT(base, mask)    (*((base)+20) &= ~(mask))
#define DIRECT_MODE_OUTPUT(base, mask)   (*((base)+20) |= (mask))
#define DIRECT_WRITE_LOW(base, mask)     (*((base)+8) = (mask))
#define DIRECT_WRITE_HIGH(base, mask)    (*((base)+4) = (mask))


#elif defined(__SAM3X8E__)
#define PIN_TO_BASEREG(pin)              (&(digitalPinToPort(pin)->PIO_PER))
#define PIN_TO_BITMASK(pin)              (digitalPinToBitMask(pin))
#define IO_REG_TYPE uint32_t
#define IO_REG_ASM
#define DIRECT_READ(base, mask)          (((*((base)+15)) & (mask)) ? 1 : 0)
#define DIRECT_MODE_INPUT(base, mask)    ((*((base)+5)) = (mask))
#define DIRECT_MODE_OUTPUT(base, mask)   ((*((base)+4)) = (mask))
#define DIRECT_WRITE_LOW(base, mask)     ((*((base)+13)) = (mask))
#define DIRECT_WRITE_HIGH(base, mask)    ((*((base)+12)) = (mask))


#elif defined(__PIC32MX__)
#define PIN_TO_BASEREG(pin)
(portModeRegister(digitalPinToPort(pin)))
#define PIN_TO_BITMASK(pin)              (digitalPinToBitMask(pin))
#define IO_REG_TYPE uint32_t
#define IO_REG_ASM
#define DIRECT_READ(base, mask)          (((*(base+4)) & (mask)) ? 1 : 0)
//PORTX + 0x10
#define DIRECT_MODE_INPUT(base, mask)    ((*(base+2)) = (mask))
//TRISXSET + 0x08
#define DIRECT_MODE_OUTPUT(base, mask)   ((*(base+1)) = (mask))
//TRISXCLR + 0x04
#define DIRECT_WRITE_LOW(base, mask)     ((*(base+8+1)) = (mask))
//LATXCLR  + 0x24
#define DIRECT_WRITE_HIGH(base, mask)    ((*(base+8+2)) = (mask))
//LATXSET + 0x28


#elif defined(ARDUINO_ARCH_ESP8266)
#define PIN_TO_BASEREG(pin) ((volatile uint32_t*) GPO)
```

```
#define PIN_TO_BITMASK(pin) (1 << pin)

#define IO_REG_TYPE uint32_t

#define IO_REG_ASM

#define DIRECT_READ(base, mask) ((GPI & (mask)) ? 1 : 0) //GPIO_IN_ADDRESS

#define DIRECT_MODE_INPUT(base, mask) (GPE &= ~(mask))
//GPIO_ENABLE_W1TC_ADDRESS

#define DIRECT_MODE_OUTPUT(base, mask) (GPE |= (mask))
//GPIO_ENABLE_W1TS_ADDRESS

#define DIRECT_WRITE_LOW(base, mask) (GPOC = (mask)) //GPIO_OUT_W1TC_ADDRESS

#define DIRECT_WRITE_HIGH(base, mask) (GPOS = (mask))
//GPIO_OUT_W1TS_ADDRESS


#elif defined(__SAMD21G18A__)
// runs extremely slow/unreliable on Arduino Zero - help wanted....
#define PIN_TO_BASEREG(pin)
portModeRegister(digitalPinToPort(pin))

#define PIN_TO_BITMASK(pin)              (digitalPinToBitMask(pin))

#define IO_REG_TYPE uint32_t

#define IO_REG_ASM

#define DIRECT_READ(base, mask)          (((*((base)+8)) & (mask)) ? 1 : 0)

#define DIRECT_MODE_INPUT(base, mask)    ((*((base)+1)) = (mask))

#define DIRECT_MODE_OUTPUT(base, mask)   ((*((base)+2)) = (mask))

#define DIRECT_WRITE_LOW(base, mask)     ((*((base)+5)) = (mask))

#define DIRECT_WRITE_HIGH(base, mask)    ((*((base)+6)) = (mask))


#elif defined(RBL_NRF51822)
#define PIN_TO_BASEREG(pin)              (0)

#define PIN_TO_BITMASK(pin)              (pin)

#define IO_REG_TYPE uint32_t

#define IO_REG_ASM

#define DIRECT_READ(base, pin)        nrf_gpio_pin_read(pin)

#define DIRECT_WRITE_LOW(base, pin)   nrf_gpio_pin_clear(pin)

#define DIRECT_WRITE_HIGH(base, pin)  nrf_gpio_pin_set(pin)

#define DIRECT_MODE_INPUT(base, pin)  nrf_gpio_cfg_input(pin,
NRF_GPIO_PIN_NOPULL)

#define DIRECT_MODE_OUTPUT(base, pin) nrf_gpio_cfg_output(pin)


#elif defined(__arc__)


#include "scss_registers.h"
```

```c
#include "portable.h"
#include "avr/pgmspace.h"


#define GPIO_ID(pin)                    (g_APinDescription[pin].ulGPIOId)
#define GPIO_TYPE(pin)                  (g_APinDescription[pin].ulGPIOType)
#define GPIO_BASE(pin)                  (g_APinDescription[pin].ulGPIOBase)
#define DIR_OFFSET_SS            0x01
#define DIR_OFFSET_SOC           0x04
#define EXT_PORT_OFFSET_SS        0x0A
#define EXT_PORT_OFFSET_SOC          0x50


/* GPIO registers base address */
#define PIN_TO_BASEREG(pin)             ((volatile uint32_t
*)g_APinDescription[pin].ulGPIOBase)
#define PIN_TO_BITMASK(pin)            pin
#define IO_REG_TYPE                    uint32_t
#define IO_REG_ASM


static inline __attribute__((always_inline))
IO_REG_TYPE directRead(volatile IO_REG_TYPE *base, IO_REG_TYPE pin)
{
    IO_REG_TYPE ret;
    if (SS_GPIO == GPIO_TYPE(pin)) {
        ret = READ_ARC_REG(((IO_REG_TYPE)base + EXT_PORT_OFFSET_SS));
    } else {
        ret = MMIO_REG_VAL_FROM_BASE((IO_REG_TYPE)base,
EXT_PORT_OFFSET_SOC);
    }
    return ((ret >> GPIO_ID(pin)) & 0x01);
}


static inline __attribute__((always_inline))
void directModeInput(volatile IO_REG_TYPE *base, IO_REG_TYPE pin)
{
    if (SS_GPIO == GPIO_TYPE(pin)) {
        WRITE_ARC_REG(READ_ARC_REG((((IO_REG_TYPE)base) + DIR_OFFSET_SS)) &
~(0x01 << GPIO_ID(pin)),
                    ((IO_REG_TYPE)(base) + DIR_OFFSET_SS));
    } else {
```

```
        MMIO_REG_VAL_FROM_BASE((IO_REG_TYPE)base, DIR_OFFSET_SOC) &= ~(0x01
<< GPIO_ID(pin));
    }
}


static inline __attribute__((always_inline))
void directModeOutput(volatile IO_REG_TYPE *base, IO_REG_TYPE pin)
{
    if (SS_GPIO == GPIO_TYPE(pin)) {
        WRITE_ARC_REG(READ_ARC_REG(((IO_REG_TYPE)(base) + DIR_OFFSET_SS)) |
(0x01 << GPIO_ID(pin)),
                      ((IO_REG_TYPE)(base) + DIR_OFFSET_SS));
    } else {
        MMIO_REG_VAL_FROM_BASE((IO_REG_TYPE)base, DIR_OFFSET_SOC) |= (0x01
<< GPIO_ID(pin));
    }
}


static inline __attribute__((always_inline))
void directWriteLow(volatile IO_REG_TYPE *base, IO_REG_TYPE pin)
{
    if (SS_GPIO == GPIO_TYPE(pin)) {
        WRITE_ARC_REG(READ_ARC_REG(base) & ~(0x01 << GPIO_ID(pin)), base);
    } else {
        MMIO_REG_VAL(base) &= ~(0x01 << GPIO_ID(pin));
    }
}
static inline __attribute__((always_inline))
void directWriteHigh(volatile IO_REG_TYPE *base, IO_REG_TYPE pin)
{
    if (SS_GPIO == GPIO_TYPE(pin)) {
        WRITE_ARC_REG(READ_ARC_REG(base) | (0x01 << GPIO_ID(pin)), base);
    } else {
        MMIO_REG_VAL(base) |= (0x01 << GPIO_ID(pin));
    }
}


#define DIRECT_READ(base, pin)          directRead(base, pin)
#define DIRECT_MODE_INPUT(base, pin)    directModeInput(base, pin)
#define DIRECT_MODE_OUTPUT(base, pin)   directModeOutput(base, pin)
```

```cpp
#define DIRECT_WRITE_LOW(base, pin)     directWriteLow(base, pin)
#define DIRECT_WRITE_HIGH(base, pin)    directWriteHigh(base, pin)
#endif


// some 3.3V chips with 5V tolerant pins need this workaround
//
#if defined(__MK20DX256__)
#define FIVE_VOLT_TOLERANCE_WORKAROUND
#endif


// library interface description
class CapacitiveSensor
{
  // user-accessible "public" interface
  public:
  // methods
      CapacitiveSensor(uint8_t sendPin, uint8_t receivePin);
      long capacitiveSensorRaw(uint8_t samples);
      long capacitiveSensor(uint8_t samples);
      void set_CS_Timeout_Millis(unsigned long timeout_millis);
      void reset_CS_AutoCal();
      void set_CS_AutocaL_Millis(unsigned long autoCal_millis);
  // library-accessible "private" interface
  private:
  // variables
      int error;
      unsigned long  leastTotal;
      unsigned int   loopTimingFactor;
      unsigned long  CS_Timeout_Millis;
      unsigned long  CS_AutocaL_Millis;
      unsigned long  lastCal;
      unsigned long  total;
      IO_REG_TYPE sBit;   // send pin's ports and bitmask
      volatile IO_REG_TYPE *sReg;
      IO_REG_TYPE rBit;    // receive pin's ports and bitmask
      volatile IO_REG_TYPE *rReg;
  // methods
      int SenseOneCycle(void);
};
```

```
#endif
```

DEV_Config.h

```
/*************************************************************************
***

***************************Hardware interface layer************************
***

* | file        :   DEV_Config.h

* | version     :   V1.0

* | date        :   2017-12-14

* | function    :

    Provide the hardware underlying interface

*************************************************************************
**/

#ifndef _DEV_CONFIG_H_

#define _DEV_CONFIG_H_


#include <Arduino.h>


#define BYTE             uint8_t

#define WORD             uint16_t


#define DEV_DEBUG 0

#if DEV_DEBUG

    #define DEBUG(__info) Serial.print(__info)

#else

    #define DEBUG(__info)

#endif
/*************************************************************************
*************

        //Use the  library function definition

*************************************************************************
*************/

//GPIO config

#define MOTOR1_A     2

#define MOTOR1_B     3

#define MOTOR1_EN    6


#define MOTOR2_A     4

#define MOTOR2_B     5
```

```
#define MOTOR2_EN    9


#define MOTOR3_A     7
#define MOTOR3_B     8
#define MOTOR3_EN    10


#define MOTOR4_A     12
#define MOTOR4_B     13
#define MOTOR4_EN    11


#define SET_PIN(__PIN, __VOL) digitalWrite(__PIN, __VOL)


/*----------------------------------------------------------------------------
----------------------------*/
uint8_t System_Init(void);
void System_Exit(void);
void DEV1_Init(void);
void DEV2_Init(void);
void Driver_Delay_ms(unsigned long xms);
void Driver_Delay_us(int xus);
#endif
```

DEV_Config.cpp

```
/**************************************************************************
***
***************************Hardware interface layer***********************
***
* | file        :   DEV_Config.cpp
* | version     :   V1.0
* | date        :   2017-12-14
* | function    :
    Provide the hardware underlying interface
**************************************************************************
**/
#include "DEV_Config.h"
/**************************************************************************
*****
function:   System Init and exit
note:
```

```
    Initialize the communication method
***************************************************************************
****/

uint8_t System_Init(void)

{

    Serial.begin(115200);

    Serial.println("GPIO Init...");


    return 0;

}



void System_Exit(void)

{

    Serial.println("Demo over...");

}



void DEV1_Init(void)

{

    //set pin output

    pinMode(MOTOR1_A,   OUTPUT);

    pinMode(MOTOR1_B,   OUTPUT);

    pinMode(MOTOR2_A,   OUTPUT);

    pinMode(MOTOR2_B,   OUTPUT);

    pinMode(MOTOR1_EN,  OUTPUT);

    pinMode(MOTOR2_EN,  OUTPUT);


    //enable L293D

    digitalWrite(MOTOR1_EN, 1);

    digitalWrite(MOTOR2_EN, 1);


    //motor1

    digitalWrite(MOTOR1_A, 1);

    digitalWrite(MOTOR1_B, 1);

    digitalWrite(MOTOR2_A, 1);

    digitalWrite(MOTOR2_B, 1);

}



void DEV2_Init(void)

{
```

```
    //set pin output
    pinMode(MOTOR3_A,   OUTPUT);
    pinMode(MOTOR3_B,   OUTPUT);
    pinMode(MOTOR4_A,   OUTPUT);
    pinMode(MOTOR4_B,   OUTPUT);
    pinMode(MOTOR3_EN,  OUTPUT);
    pinMode(MOTOR4_EN,  OUTPUT);


    //enable L293D
    digitalWrite(MOTOR3_EN, 1);
    digitalWrite(MOTOR4_EN, 1);


    //motor2
    digitalWrite(MOTOR3_A, 1);
    digitalWrite(MOTOR3_B, 1);
    digitalWrite(MOTOR4_A, 1);
    digitalWrite(MOTOR4_B, 1);
}


/*****************************************************************************
*****
function:   Delay function
note:
    Driver_Delay_ms(xms) : Delay x ms
    Driver_Delay_us(xus) : Delay x us
*****************************************************************************
****/
void Driver_Delay_ms(unsigned long xms)
{
    delay(xms);
}


void Driver_Delay_us(int xus)
{
    for(int j=xus; j > 0; j--);
}
```

Motor.h

```
/*****************************************************************************
***

**************************Intermediate driver layer**********************
***

* | file        :   Motor.h

* | version     :   V1.0

* | date        :   2017-12-14

* | function    :   28BYJ-48 Stepper motor Drive function

*****************************************************************************
**/
#ifndef __MOTOR_H
#define __MOTOR_H


#include "DEV_Config.h"


//define two devices
#define MOTOR_DEV_1  1
#define MOTOR_DEV_2  2


struct MOTOR{
    BYTE L1;    //Orange line
    BYTE L2;    //Yellow line
    BYTE L3;    //Powder line
    BYTE L4;    //Blue line
};


/*****************************************************************************
*****

  function:

            Macro definition variable name
*****************************************************************************
****/
void Motor_Init(BYTE Motor1, BYTE Motor2);
void Motor_Trun(BYTE Motor, unsigned long Angle, int dir);
#endif
```

Motor.cpp

```
/*****************************************************************************
***
```

```
****************************Intermediate driver layer************************
***
* | file        :   Motor.cpp
* | version     :   V1.0
* | date        :   2017-12-14
* | function    :   28BYJ-48 Stepper motor Drive function
*****************************************************************************
**/
#include "Motor.h"
struct MOTOR sMotor1, sMotor2;


BYTE BeatCode[8] = { //Stepper motor eight eight beat code
    0x0E, 0x0C, 0x0D, 0x09, 0x0B, 0x03, 0x07, 0x06
};


static void Motor_Setbit(struct MOTOR sMotor,BYTE Data)
{
    BYTE Bit[4] = {sMotor.L1, sMotor.L2, sMotor.L3, sMotor.L4};
    Data = (~Data) & 0x0f;


    BYTE Temp;
    for(Temp = 0;Temp < 4; Temp++){
        if(Data & 0x01 == 1){
            DEBUG(" 0 ");
            SET_PIN(Bit[Temp], 0);
        }else{
            DEBUG(" 1 ");
            SET_PIN(Bit[Temp], 1);
        }
        Data = Data >> 1;
    }
  Driver_Delay_ms(2);
    DEBUG("\r\n");
}
void Motor_Trun(BYTE Motor_dev, unsigned long Angle, int dir)
{
    struct MOTOR sMotor;
    if(Motor_dev == MOTOR_DEV_1){
        sMotor = sMotor1;
    }else if(Motor_dev == MOTOR_DEV_2){
```

```c
        sMotor = sMotor2;
    }else{
        DEBUG("not motor device \r\n");
    }


    BYTE Index = 0;
    unsigned long beats = (Angle * 4076) / 360 ; //Need to turn the beat
    //unsigned long beatsmax = (Angle * 4076) / 360 ;
  for(beats = beats; beats > 0; beats--){
//  for(beats = 0; beats < beatsmax; beats++){
        if( dir==0){
    Motor_Setbit(sMotor, BeatCode[Index]);
        }else{
        Motor_Setbit(sMotor, BeatCode[7-Index]);
        }
        Index++;
        if(Index % 8 == 0){
            Index = Index & 0x07; //Greater than 8 clear 0
            DEBUG("***************\r\n");
        }
    }
    Motor_Setbit(sMotor, 0x0f);
}


void Motor_Init(BYTE Motor1_dev, BYTE Motor2_dev)
{
    if(Motor1_dev == MOTOR_DEV_1){
        DEV1_Init();

        sMotor1.L1 = MOTOR1_A;
        sMotor1.L2 = MOTOR1_B;
        sMotor1.L3 = MOTOR2_A;
        sMotor1.L4 = MOTOR2_B;
    }


    if(Motor2_dev == MOTOR_DEV_2){
        DEV2_Init();

        sMotor2.L1 = MOTOR3_A;
```

```
        sMotor2.L2 = MOTOR3_B;

        sMotor2.L3 = MOTOR4_A;

        sMotor2.L4 = MOTOR4_B;

    }

}
```

Bibliography

[1]   E. Φραγκιάδης *et al.*, "ΕΡΓΑΛΕΙΑ ΣΤΗ ΛΑΠΑΡΟΣΚΟΠΙΚΗ-ΡΟΜΠΟΤΙΚΗ ΧΕΙΡΟΥΡΓΙΚΗ ΣΤΗΝ ΟΥΡΟΛΟΓΙΑ."

[2]   N. Enayati, E. De Momi, and G. Ferrigno, "Haptics in Robot-Assisted Surgery: Challenges and Benefits," *IEEE Rev. Biomed. Eng.*, vol. 9, pp. 49–65, 2016, doi: 10.1109/rbme.2016.2538080.

[3]   M. I. Tiwana, S. J. Redmond, and N. H. Lovell, "A review of tactile sensing technologies with applications in biomedical engineering," *Sensors Actuators A Phys.*, vol. 179, pp. 17–31, Jun. 2012, doi: 10.1016/j.sna.2012.02.051.

[4]   E. P. W. van der Putten, R. H. M. Goossens, J. J. Jakimowicz, and J. Dankelman, "Haptics in minimally invasive surgery - A review," *Minimally Invasive Therapy and Allied Technologies*, vol. 17, no. 1. Minim Invasive Ther Allied Technol, pp. 3–16, 2008, doi: 10.1080/13645700701820242.

[5]   G. Tholey, J. P. Desai, and A. E. Castellanos, "Force Feedback Plays a Significant Role in Minimally Invasive Surgery," *Ann. Surg.*, vol. 241, no. 1, Jan. 2005, doi: 10.1097/01.sla.0000149301.60553.1e.

[6]   B. Hakim and Basari, "Tuberculosis detection analysis using texture features on CXRs images," 2019, doi: 10.1063/1.5096734.

[7]   S. Ravimohan, H. Kornfeld, D. Weissman, and G. P. Bisson, "Tuberculosis and lung damage: from epidemiology to pathophysiology," *Eur. Respir. Rev.*, vol. 27, no. 147, p. 170077, Feb. 2018, doi: 10.1183/16000617.0077-2017.

[8]   R. L. Hunter, "Pathology of post primary tuberculosis of the lung: An illustrated critical review," *Tuberculosis*, vol. 91, no. 6, pp. 497–509, Nov. 2011, doi: 10.1016/j.tube.2011.03.007.

[9]   R. Long, B. Maycher, A. Dhar, J. Manfreda, E. Hershfield, and N. Anthonisen, "Pulmonary tuberculosis treated with directly observed therapy: Serial changes in lung structure and function," *Chest*, vol. 113, no. 4, pp. 933–943, 1998, doi: 10.1378/chest.113.4.933.

[10]   Y. D. Cid, O. Jimenez-del-Toro, P.-A. Poletti, and H. Müller, "A Graph Model of the Lungs with Morphology-Based Structure for Tuberculosis Type Classification," in *Lecture Notes in Computer Science*, Springer International Publishing, 2019, pp. 372–383.

[11]   H. Liu, Y. Shao, D. Guo, Y. Zheng, Z. Zhao, and T. Qiu, "Cirrhosis Classification Based on Texture Classification of Random Features," *Comput. Math. Methods Med.*, vol. 2014, pp. 1–8, 2014, doi: 10.1155/2014/536308.

[12]   E. J. Heathcote, "Primary biliary cirrhosis: historical perspective," *Clin. Liver Dis.*, vol. 7, no. 4, pp. 735–740, Nov. 2003, doi: 10.1016/s1089-3261(03)00098-9.

[13]   C. C. Giallourakis, P. M. Rosenberg, and L. S. Friedman, "The liver in heart failure," *Clin. Liver Dis.*, vol. 6, no. 4, pp. 947–967, Nov. 2002, doi: 10.1016/s1089-3261(02)00056-9.

[14]   "Pancreatic Cancer Early Detection, Diagnosis, and Staging," doi:

10.1016/j.gtc.2016.04.003.

[15] A. Borbély *et al.*, "Cardiomyocyte stiffness in diastolic heart failure," *Circulation*, vol. 111, no. 6, pp. 774–781, Feb. 2005, doi: 10.1161/01.CIR.0000155257.33485.6D.

[16] "Cardiomyopathy - NHS." https://www.nhs.uk/conditions/cardiomyopathy/ (accessed Feb. 24, 2021).

[17] A. Mojra, S. Najarian, S. M. Towliat Kashani, F. Panahi, and M. Yaghmaei, "A novel haptic robotic viscogram for characterizing the viscoelastic behaviour of breast tissue in clinical examinations," *Int. J. Med. Robot. Comput. Assist. Surg.*, vol. 7, no. 3, pp. 282–292, Sep. 2011, doi: 10.1002/rcs.396.

[18] A. Mojra, S. Najarian, S. M. Towliat Kashani, F. Panahi, and M. A. Tehrani, "A novel robotic tactile mass detector with application in clinical breast examination," *Minim. Invasive Ther. Allied Technol.*, vol. 21, no. 3, May 2012, doi: 10.3109/13645706.2011.602087.

[19] E. Afshari, S. Najarian, N. Simforoosh, and S. Hajizade Farkoush, "Design and fabrication of a novel tactile sensory system applicable in artificial palpation," *Minim. Invasive Ther. Allied Technol.*, vol. 20, no. 1, pp. 22–29, Jan. 2011, doi: 10.3109/13645706.2010.518739.

[20] A. A. Mehrizi, S. Najarian, R. Khodambashi, and S. Dehkhoda, "A novel method of tactile assessment of arteries using computational approach," Aug. 2018, Accessed: Dec. 15, 2020. [Online]. Available: http://arxiv.org/abs/1808.02888.

[21] A. Abouei Mehrizi, M. Moini, E. Afshari, J. Kadkhodapour, A. Sadjadian, and S. Najarian, "Application of artificial palpation in vascular surgeries for detection of peripheral arterial stenosis," *J. Med. Eng. Technol.*, vol. 38, no. 4, pp. 169–178, 2014, doi: 10.3109/03091902.2014.891663.

[22] M. Li, S. Luo, T. Nanayakkara, L. D. Seneviratne, P. Dasgupta, and K. Althoefer, "Multi-fingered haptic palpation using pneumatic feedback actuators," *Sensors Actuators A Phys.*, vol. 218, pp. 132–141, Oct. 2014, doi: 10.1016/j.sna.2014.08.003.

[23] A. Hamed *et al.*, "Advances in Haptics, Tactile Sensing, and Manipulation for Robot-Assisted Minimally Invasive Surgery, Noninvasive Surgery, and Diagnosis," *J. Robot.*, vol. 2012, pp. 1–14, 2012, doi: 10.1155/2012/412816.

[24] M. El Boghdady and A. Alijani, "Feedback in surgical education," *Surg.*, vol. 15, no. 2, pp. 98–103, Apr. 2017, doi: 10.1016/j.surge.2016.06.006.

[25] H. Schwaibold, F. Wiesend, and C. Bach, "The age of robotic surgery Is laparoscopy dead?," *Arab J. Urol.*, vol. 16, no. 3, pp. 262–269, Sep. 2018, doi: 10.1016/j.aju.2018.07.003.

[26] B. Kuebler, U. Seibold, and G. Hirzinger, "Development of actuated and sensor integrated forceps for minimally invasive robotic surgery," *Int. J. Med. Robot. Comput. Assist. Surg.*, vol. 01, no. 03, p. 96, 2005, doi: 10.1581/mrcas.2005.010305.

[27] U. Seibold, B. Kuebler, and G. Hirzinger, "Prototypic Force Feedback Instrument for Minimally Invasive Robotic Surgery," in *Medical Robotics*, I-

Tech Education and Publishing, 2008.

[28] B. S. Peters, P. R. Armijo, C. Krause, S. A. Choudhury, and D. Oleynikov, "Review of emerging surgical robotic technology," *Surg. Endosc.*, vol. 32, no. 4, pp. 1636–1655, Feb. 2018, doi: 10.1007/s00464-018-6079-2.

[29] D. K. Kim and K. H. Rha, "Supporting evidence for robotic urological surgery," *Korean J. Urol.*, vol. 56, no. 11, p. 733, 2015, doi: 10.4111/kju.2015.56.11.733.

[30] R. Nakadate, J. Arata, and M. Hashizume, "Next-generation robotic surgery - from the aspect of surgical robots developed by industry," *Minim. Invasive Ther. Allied Technol.*, vol. 24, no. 1, pp. 2–7, Jan. 2015, doi: 10.3109/13645706.2014.1003140.

[31] S. De, L. M. Seltz, and S. D. Herrell, "Emerging Molecular, Imaging and Technological Advances in the Field of Robotic Surgery," in *Robotics in Genitourinary Surgery*, Springer International Publishing, 2018, pp. 909–925.

[32] M. G. Medina, S. S. Tsoraides, and A. M. Dwyer, "Review and update: robotic transanal surgery (RTAS)," *Updates Surg.*, vol. 70, no. 3, pp. 369–374, Aug. 2018, doi: 10.1007/s13304-018-0580-y.

[33] E. D. C. Subido, D. M. M. Pacis, and N. T. Bugtai, "Recent technological advancements in laparoscopic surgical instruments," 2018, doi: 10.1063/1.5023977.

[34] A. Navaratnam, H. Abdul-Muhsin, and M. Humphreys, "Updates in Urologic Robot Assisted Surgery," *F1000Research*, vol. 7, p. 1948, Dec. 2018, doi: 10.12688/f1000research.15480.1.

[35] K. R. Sheth and C. J. Koh, "The Future of Robotic Surgery in Pediatric Urology: Upcoming Technology and Evolution Within the Field," *Front. Pediatr.*, vol. 7, Jul. 2019, doi: 10.3389/fped.2019.00259.

[36] R. Nakadate and M. Hashizume, "Intelligent Information-Guided Robotic Surgery," in *Recent Advances in Laparoscopic Surgery [Working Title]*, IntechOpen, 2018.

[37] B. P. M. Yeung and T. Gourlay, "A technical review of flexible endoscopic multitasking platforms," *Int. J. Surg.*, vol. 10, no. 7, pp. 345–354, 2012, doi: 10.1016/j.ijsu.2012.05.009.

[38] P. P. Rao, "Robotic surgery: new robots and finally some real competition!," *World J. Urol.*, vol. 36, no. 4, pp. 537–541, Feb. 2018, doi: 10.1007/s00345-018-2213-y.

[39] J. J. Rassweiler, A. S. Goezen, J. Klein, and E. Liatsikos, "New Robotic Platforms," *Robot. Urol.*, pp. 3–38, 2018.

[40] "avatera system - avateramedical." https://www.avatera.eu/en/avatera-system (accessed Mar. 28, 2021).

[41] V. Ozben *et al.*, "Is da Vinci Xi better than da Vinci Si in robotic rectal cancer surgery? Comparison of the 2 generations of da Vinci Systems," *Surg. Laparosc. Endosc. Percutaneous Tech.*, vol. 26, no. 5, pp. 417–423, Jul. 2016, doi: 10.1097/SLE.0000000000000320.

[42] J. Ngu, C. Tsang, and D. Koh, "The da Vinci Xi: a review of its capabilities, versatility, and potential role in robotic colorectal surgery," *Robot. Surg. Res. Rev.*, vol. Volume 4, pp. 77–85, Jul. 2017, doi: 10.2147/rsrr.s119317.

[43] K. D. Chang, A. A. Raheem, and K. H. Rha3, "Novel robotic systems and future directions," *Indian J Urol*, vol. 34, no. 2, pp. 110–114, 2018.

[44] C. Freschi, V. Ferrari, F. Melfi, M. Ferrari, F. Mosca, and A. Cuschieri, "Technical review of the da Vinci surgical telemanipulator," *Int. J. Med. Robot. Comput. Assist. Surg.*, vol. 9, no. 4, pp. 396–406, Nov. 2012, doi: 10.1002/rcs.1468.

[45] U. Hagn *et al.*, "DLR MiroSurge: a versatile system for research in endoscopic telesurgery," *Int. J. Comput. Assist. Radiol. Surg.*, vol. 5, no. 2, pp. 183–193, Jun. 2009, doi: 10.1007/s11548-009-0372-4.

[46] R. Konietschke *et al.*, "The DLR MiroSurge-A Robotic System for Surgery," doi: 10.1108/01439910810876427.

[47] A. A. Raheem *et al.*, "Robot-assisted Fallopian tube transection and anastomosis using the new REVO-I robotic surgical system: feasibility in a chronic porcine model," *BJU Int.*, vol. 118, no. 4, pp. 604–609, May 2016, doi: 10.1111/bju.13517.

[48] J. Lim, W. Lee, D. Park, H. Yea, S. Kim, and C. Kang, "Robotic cholecystectomy using Revo-i Model MSR-5000, the newly developed Korean robotic surgical system: a preclinical study," *Surg. Endosc.*, vol. 31, Dec. 2017, doi: 10.1007/s00464-016-5357-0.

[49] D. K. Kim, D. W. Park, and K. H. Rha, "Robot-assisted Partial Nephrectomy with the REVO-I Robot Platform in Porcine Models," *Eur. Urol.*, vol. 69, no. 3, pp. 541–542, Mar. 2016, doi: 10.1016/j.eururo.2015.11.024.

[50] B. Seeliger, M. Diana, J. P. Ruurda, K. M. Konstantinidis, J. Marescaux, and L. L. Swanström, "Enabling single-site laparoscopy: the SPORT platform," *Surg. Endosc.*, vol. 33, no. 11, pp. 3696–3703, Jan. 2019, doi: 10.1007/s00464-018-06658-x.

[51] "Triboelectric Generator Produces Electricity by Harnessing Frictional Forces | Research Horizons | Georgia Tech's Research News." https://rh.gatech.edu/news/139511/triboelectric-generator-produces-electricity-harnessing-frictional-forces (accessed Mar. 28, 2021).

[52] M. E. Karagozler, I. Poupyrev, G. K. Fedder, and Y. Suzuki, "Paper generators: Harvesting energy from touching, rubbing and sliding," in *UIST 2013 - Proceedings of the 26th Annual ACM Symposium on User Interface Software and Technology*, 2013, pp. 23–30, doi: 10.1145/2501988.2502054.

[53] W. Li, D. Torres, T. Wang, C. Wang, and N. Sepúlveda, "Flexible and biocompatible polypropylene ferroelectret nanogenerator (FENG): On the path toward wearable devices powered by human motion," *Nano Energy*, vol. 30, pp. 649–657, Dec. 2016, doi: 10.1016/j.nanoen.2016.10.007.

[54] W. Seung *et al.*, "Nanopatterned textile-based wearable triboelectric nanogenerator," *ACS Nano*, vol. 9, no. 4, pp. 3501–3509, Apr. 2015, doi: 10.1021/nn507221f.

[55] C. Wu, T. W. Kim, F. Li, and T. Guo, "Wearable Electricity Generators Fabricated Utilizing Transparent Electronic Textiles Based on Polyester/Ag Nanowires/Graphene Core-Shell Nanocomposites," *ACS Nano*, vol. 10, no. 7, pp. 6449–6457, Jul. 2016, doi: 10.1021/acsnano.5b08137.

[56] F. J. S. D. A. & C. S. R. Holler, *Principles of Instrumental Analysis*, 6th ed. Cengage Learning, 2007.

[57] C. García Núñez, L. Manjakkal, and R. Dahiya, "Energy autonomous electronic skin," *npj Flexible Electronics*, vol. 3, no. 1. Nature Research, Dec. 01, 2019, doi: 10.1038/s41528-018-0045-x.

[58] M. Kalantari, M. Ramezanifard, R. Ahmadi, J. Dargahi, and J. Kövecses, "A piezoresistive tactile sensor for tissue characterization during catheter-based cardiac surgery," *Int. J. Med. Robot. Comput. Assist. Surg.*, vol. 7, no. 4, pp. 431–440, Dec. 2011, doi: 10.1002/rcs.413.

[59] Z. Li and C. S. H. Ng, "Latest technology in minimally invasive thoracic surgery," *Ann. Transl. Med.*, vol. 7, no. 2, pp. 35–35, Jan. 2019, doi: 10.21037/atm.2018.12.47.

[60] A. Abiri *et al.*, "Artificial palpation in robotic surgery using haptic feedback," *Surg. Endosc.*, vol. 33, no. 4, pp. 1252–1259, Apr. 2019, doi: 10.1007/s00464-018-6405-8.

[61] N. M. Bandari, R. Ahmadi, A. Hooshiar, J. Dargahi, and M. Packirisamy, "Hybrid piezoresistive-optical tactile sensor for simultaneous measurement of tissue stiffness and detection of tissue discontinuity in robot-assisted minimally invasive surgery," *J. Biomed. Opt.*, vol. 22, no. 7, p. 077002, Jul. 2017, doi: 10.1117/1.jbo.22.7.077002.

[62] Y. Zhang, F. Ju, X. Wei, D. Wang, and Y. Wang, "A Piezoelectric Tactile Sensor for Tissue Stiffness Detection with Arbitrary Contact Angle," *Sensors*, vol. 20, no. 22, Nov. 2020, doi: 10.3390/s20226607.

[63] Y. Yun *et al.*, "A resonant tactile stiffness sensor for lump localization in robot-assisted minimally invasive surgery," *Proc. Inst. Mech. Eng. Part H J. Eng. Med.*, vol. 233, no. 9, pp. 909–920, Sep. 2019, doi: 10.1177/0954411919856519.

[64] M. Beccani, C. Di Natali, L. J. Sliker, J. A. Schoen, M. E. Rentschler, and P. Valdastri, "Wireless tissue palpation for intraoperative detection of lumps in the soft tissue," *IEEE Trans. Biomed. Eng.*, vol. 61, no. 2, pp. 353–361, Feb. 2014, doi: 10.1109/TBME.2013.2279337.

[65] H. Mattila, "Yarn to Fabric: Intelligent Textiles," in *Textiles and Fashion: Materials, Design and Technology*, Elsevier Inc., 2015, pp. 355–376.

[66] Z. He *et al.*, "Highly stretchable multi-walled carbon nanotube/thermoplastic polyurethane composite fibers for ultrasensitive, wearable strain sensors," *Nanoscale*, vol. 11, no. 13, pp. 5884–5890, 2019, doi: 10.1039/C9NR01005J.

[67] H. Souri and D. Bhattacharyya, "Highly Stretchable Multifunctional Wearable Devices Based on Conductive Cotton and Wool Fabrics," *ACS Appl. Mater. Interfaces*, vol. 10, no. 24, pp. 20845–20853, Jun. 2018, doi: 10.1021/acsami.8b04775.

[68] O. Atalay, "Textile-Based, Interdigital, Capacitive, Soft-Strain Sensor for Wearable Applications," *Materials (Basel).*, vol. 11, no. 5, p. 768, May 2018, doi: 10.3390/ma11050768.

[69] C. Gonçalves, A. Ferreira da Silva, J. Gomes, and R. Simoes, "Wearable E-Textile Technologies: A Review on Sensors, Actuators and Control Elements," *Inventions*, vol. 3, no. 1, p. 14, Mar. 2018, doi: 10.3390/inventions3010014.

[70] K. Liu *et al.*, "Polyaniline nanofiber wrapped fabric for high performance flexible pressure sensors," *Polymers (Basel).*, vol. 11, no. 7, 2019, doi: 10.3390/polym11071120.

[71] Z. Zhou *et al.*, "Supersensitive all-fabric pressure sensors using printed textile electrode arrays for human motion monitoring and human-machine interaction," *J. Mater. Chem. C*, vol. 6, no. 48, pp. 13120–13127, 2018, doi: 10.1039/c8tc02716a.

[72] A. Kiaghadi, M. Baima, J. Gummeson, T. Andrew, and D. Ganesan, "Fabric as a Sensor: Towards unobtrusive sensing of human behavior with triboelectric textiles," in *SenSys 2018 - Proceedings of the 16th Conference on Embedded Networked Sensor Systems*, Nov. 2018, pp. 199–210, doi: 10.1145/3274783.3274845.

[73] J. Ren *et al.*, "Environmentally-friendly conductive cotton fabric as flexible strain sensor based on hot press reduced graphene oxide," *Carbon N. Y.*, vol. 111, Jan. 2017, doi: 10.1016/j.carbon.2016.10.045.

[74] O. Atalay, A. Atalay, J. Gafford, and C. Walsh, "A Highly Sensitive Capacitive-Based Soft Pressure Sensor Based on a Conductive Fabric and a Microporous Dielectric Layer," *Adv. Mater. Technol.*, vol. 3, no. 1, Jan. 2018, doi: 10.1002/admt.201700237.

[75] B. Choi *et al.*, "Highly Conductive Fiber with Waterproof and Self-Cleaning Properties for Textile Electronics," *ACS Appl. Mater. Interfaces*, vol. 10, no. 42, pp. 36094–36101, Oct. 2018, doi: 10.1021/acsami.8b10217.

[76] Z. Ma, R. Xu, W. Wang, and D. Yu, "A wearable, anti-bacterial strain sensor prepared by silver plated cotton/spandex blended fabric for human motion monitoring," *Colloids Surfaces A Physicochem. Eng. Asp.*, vol. 582, p. 123918, Dec. 2019, doi: 10.1016/j.colsurfa.2019.123918.

[77] Z. Tang *et al.*, "Highly conductive, washable and super-hydrophobic wearable carbon nanotubes e-textile for vacuum pressure sensors," *Sensors Actuators, A Phys.*, vol. 303, p. 111710, Mar. 2020, doi: 10.1016/j.sna.2019.111710.

[78] S. J. Kim *et al.*, "High Durability and Waterproofing rGO/SWCNT-Fabric-Based Multifunctional Sensors for Human-Motion Detection," *ACS Appl. Mater. Interfaces*, vol. 10, no. 4, pp. 3921–3928, Jan. 2018, doi: 10.1021/acsami.7b15386.

[79] Y. Hirai, Y. Suzuki, T. Tsuji, and T. Watanabe, "Tough, bendable and stretchable tactile sensors array for covering robot surfaces," in *2018 IEEE International Conference on Soft Robotics, RoboSoft 2018*, Jul. 2018, pp. 276–281, doi: 10.1109/ROBOSOFT.2018.8404932.

[80] X. Duan, S. Taurand, and M. Soleimani, "Artificial skin through super-sensing

method and electrical impedance data from conductive fabric with aid of deep learning," *Sci. Rep.*, vol. 9, no. 1, Dec. 2019, doi: 10.1038/s41598-019-45484-6.

[81] D. Chen, Y. Cai, and M.-C. Huang, "Customizable Pressure Sensor Array: Design and Evaluation," *IEEE Sens. J.*, vol. 18, no. 15, Aug. 2018, doi: 10.1109/JSEN.2018.2832129.

[82] K. Ishac and K. Suzuki, "LifeChair: A Conductive Fabric Sensor-Based Smart Cushion for Actively Shaping Sitting Posture," *Sensors*, vol. 18, no. 7, Jul. 2018, doi: 10.3390/s18072261.

[83] H. E. Lee *et al.*, "Novel Electronics for Flexible and Neuromorphic Computing," *Adv. Funct. Mater.*, vol. 28, no. 32, p. 1801690, Jul. 2018, doi: 10.1002/adfm.201801690.

[84] S. Patra, R. Choudhary, R. Madhuri, and P. K. Sharma, "Graphene-Based Portable, Flexible, and Wearable Sensing Platforms: An Emerging Trend for Health Care and Biomedical Surveillance," in *Graphene Bioelectronics*, Elsevier Inc., 2018, pp. 307–338.

[85] H. Lee *et al.*, "Wearable/disposable sweat-based glucose monitoring device with multistage transdermal drug delivery module," *Sci. Adv.*, vol. 3, no. 3, Mar. 2017, doi: 10.1126/sciadv.1601314.

[86] M. S. Mannoor *et al.*, "Graphene-based wireless bacteria detection on tooth enamel," *Nat. Commun.*, vol. 3, no. 1, Jan. 2012, doi: 10.1038/ncomms1767.

[87] Y. Kanellopoulos *et al.*, "Code Quality Evaluation Methodology Using The ISO/IEC 9126 Standard," doi: 10.5121/ijsea.2010.1302.

[88] D. J. Balazs *et al.*, "Inhibition of bacterial adhesion on PVC endotracheal tubes by RF-oxygen glow discharge, sodium hydroxide and silver nitrate treatments," *Biomaterials*, vol. 25, no. 11, pp. 2139–2151, 2004, doi: 10.1016/j.biomaterials.2003.08.053.

[89] N. Stobie *et al.*, "Prevention of Staphylococcus epidermidis biofilm formation using a low-temperature processed silver-doped phenyltriethoxysilane sol-gel coating," *Biomaterials*, vol. 29, no. 8, pp. 963–969, Mar. 2008, doi: 10.1016/j.biomaterials.2007.10.057.

[90] R. Xu *et al.*, "A flexible, conductive and simple pressure sensor prepared by electroless silver plated polyester fabric," *Colloids Surfaces A Physicochem. Eng. Asp.*, vol. 578, p. 123554, Oct. 2019, doi: 10.1016/j.colsurfa.2019.04.096.

[91] Y. Mi, Y. Chan, D. Trau, P. Huang, and E. Chen, "Micromolding of PDMS scaffolds and microwells for tissue culture and cell patterning: A new method of microfabrication by the self-assembled micropatterns of diblock copolymer micelles," *Polymer (Guildf).*, vol. 47, no. 14, pp. 5124–5130, Jun. 2006, doi: 10.1016/j.polymer.2006.04.063.

[92] N. Q. Balaban *et al.*, "Force and focal adhesion assembly: A close relationship studied using elastic micropatterned substrates," *Nat. Cell Biol.*, vol. 3, no. 5, pp. 466–472, 2001, doi: 10.1038/35074532.

[93] A. S. Naidu, R. V. Patel, and M. D. Naish, "Low-Cost Disposable Tactile Sensors for Palpation in Minimally Invasive Surgery," *IEEE/ASME Trans.*

Mechatronics, vol. 22, no. 1, pp. 127–137, Feb. 2017, doi: 10.1109/TMECH.2016.2623743.